

Fine Structure of Hepatocytes During the Etiology of Several Common Pathologies

ZSUZSA SCHAFF AND KAROLY LAPIS

First Institute of Pathology and Experimental Cancer Research, Semmelweis Medical University, Budapest, Hungary, 1085

KEY WORDS Ultrastructure, Liver disease, Hepatitis, Alcoholic injury, Storage diseases

ABSTRACT Hepatocytes respond to injury by a few basic pathological reactions that are reflected in cell death, different types of degeneration, regeneration, or tumorous transformation. At the ultrastructural level, alterations of cell organelles can be observed in different combinations as a result of the injury, depending on the etiological agent(s) or pathological conditions developed. Nuclear bodies, dilation and fragmentation of rough endoplasmic reticulum (rer), swelling of mitochondria, and an increased number of lysosomes occur during acute viral hepatitis. The core and surface components of the hepatitis B virus can be localized in the liver cells in chronic hepatitis and in carriers. Close contact of hepatocytic and lymphocytic cell membranes were observed in chronic active hepatitis. Hepatocytes surrounded by an increased amount of collagen fibers are characteristic of cirrhosis. Loosely arranged, fine fibrils or condensed forms of Mallory bodies are pathognomonic for alcoholic injury. A wide spectrum of alterations are noted after drug treatment: the proliferation of smooth endoplasmic reticulum (ser) as an adaptive phenomenon, focal or complete necrosis of the cell, inflammation, and the like. The fine structural analysis of hepatocytic inclusions in storage diseases has a differential diagnostic value. The storage of copper and other elements can be measured by x-ray microanalysis. The study of the hepatocytic differentiation in liver tumors is highly important in establishing the diagnosis and in proving the hepatocytic origin of the tumor.

INTRODUCTION

With the help of electron microscopy, agents causing hepatic diseases, for example, components of hepatitis B virus and cytomegalovirus can be recognized (Phillips et al., '87). Typical nuclear alterations, such as an increase in the number of nuclear bodies, formation of nuclear inclusions, and variations in size and organization of nucleoli can be observed as a sign of acute hepatitis (Lapis and Schaff, '79). Ultrastructural analysis of cytoplasmic inclusions occurring during several liver pathologies might help in understanding the pathogenesis of certain liver diseases (Popper, '86; Popper and Schaffner, '63). This chapter will consider the fine structure of human hepatocytes in relation to the alterations in liver diseases. A brief outline of the ultrastructural features of normal hepatocytes, with reference to previous publications that provide further details, is given.

NORMAL HEPATOCYTES

There are several reports that summarize the more recent data on normal liver cell structure and function (Arias et al., '82; Lapis, '79a; MacSween and Scuthorne, '87; Motta and Fujita, '78; Phillips et al., '87).

The polyhedral hepatocytes measuring ~25 μm in diameter (Phillips et al., '87; Rouiller, '57) are arranged in trabecules that form lobules or acini (Rappaport et al., '54; Figs. 1A, 1B), and their surfaces can be easily recognized on scanning and transmission electron micrographs (Figs. 1A, 1B). The sinusoidal surface (Figs. 1A, 1B) and the bile canalculus (Figs. 2A, 2B) are

covered with microvilli. The membrane of bile canalicular microvilli expresses several enzyme activities such as that of Mg^{2+} -adenosine triphosphatase (Figs. 2C, 2D) or alkaline phosphatase. The two hemicanaluli of neighboring hepatocytes are sealed by tight junctions and form the bile canalculus (Desmet, '87).

The round or oval nuclei of the hepatocytes measure ~10 μm in diameter and have one or more nucleoli (Fig. 1B). An abundance of cytoplasm filled with organelles is characteristic of the hepatocytes. The endoplasmic reticulum consists of two continuous parts, the rough endoplasmic reticulum (rer) (Fig. 3A) and the smooth endoplasmic reticulum (ser), where several enzyme activities are located, for example, glucuronide transferase and glucose-6-phosphatase (Fig. 3B). The parallel saccules and cisternae of the Golgi complex are located near the bile canalicular surface of the hepatocytes. The lysosomes and peroxisomes appear as "dense bodies" and contain several metabolic enzymes such as acid hydrolases and catalase (Fig. 1B). An increase in the number of secondary lysosomes is very common, as a result of cell injury.

The mitochondria are the most numerous organelle in the hepatocytes; they measure ~0.5 \times 1 μm and are

Received February 15, 1988; accepted in revised form June 1, 1988.

Address reprint requests to Zsuzsa Schaff, M.D., First Institute of Pathology and Experimental Cancer Research, Semmelweis Medical University, Ullo str. 26, Budapest, Hungary, 1085.

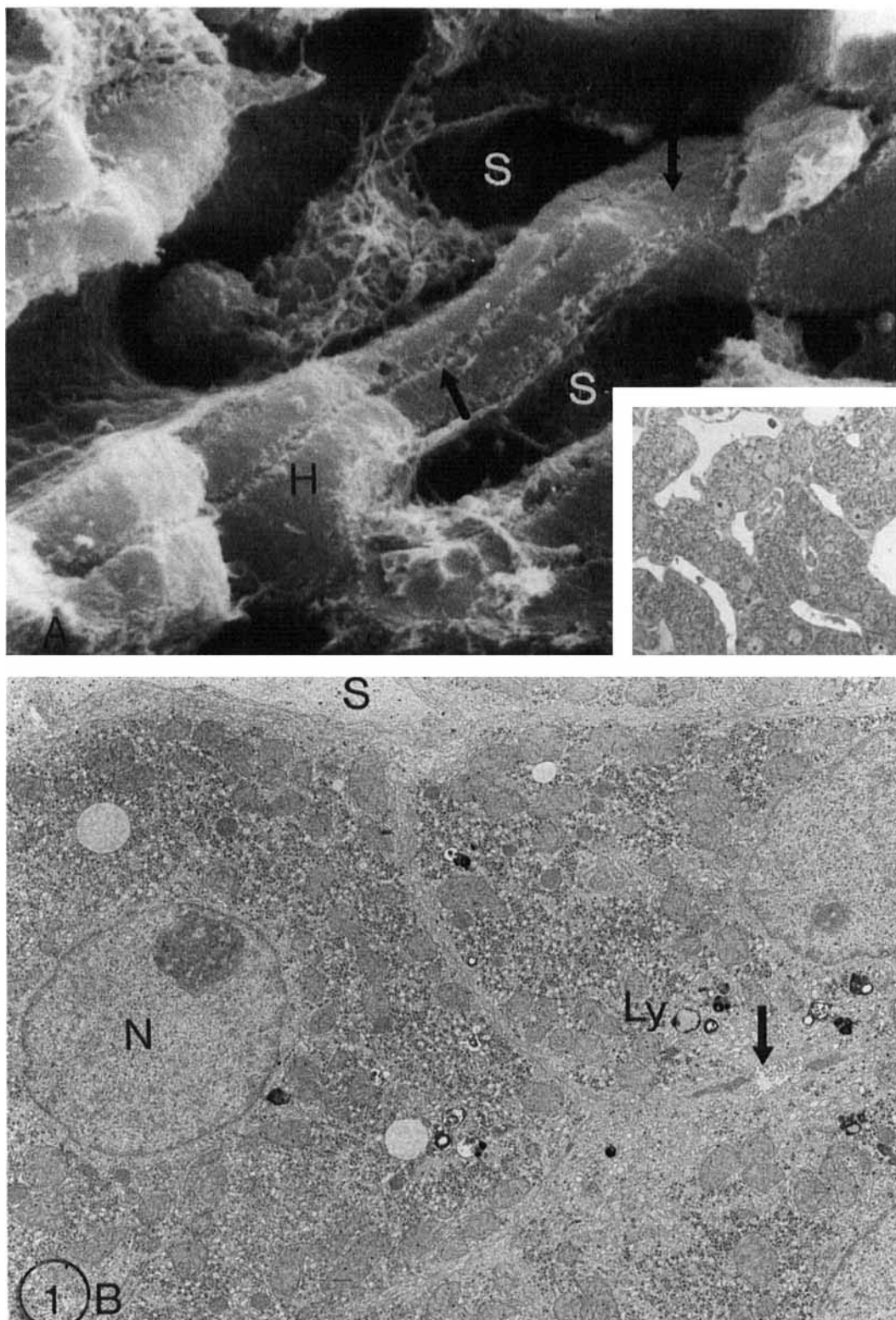


Fig. 1. Normal human liver. **A:** Scanning electron micrograph showing hepatocytes (H), sinusoids (S), and bile canaliculi (arrow). The endothelium outlines the sinusoid (S). **A:** $\times 2,000$; **Inset:** Semithin section. **B:** Transmission electron micrograph of hepatocytes with round nuclei (N), lysosomes (Ly), and bile canalculus (arrow). **B:** $\times 3,500$.

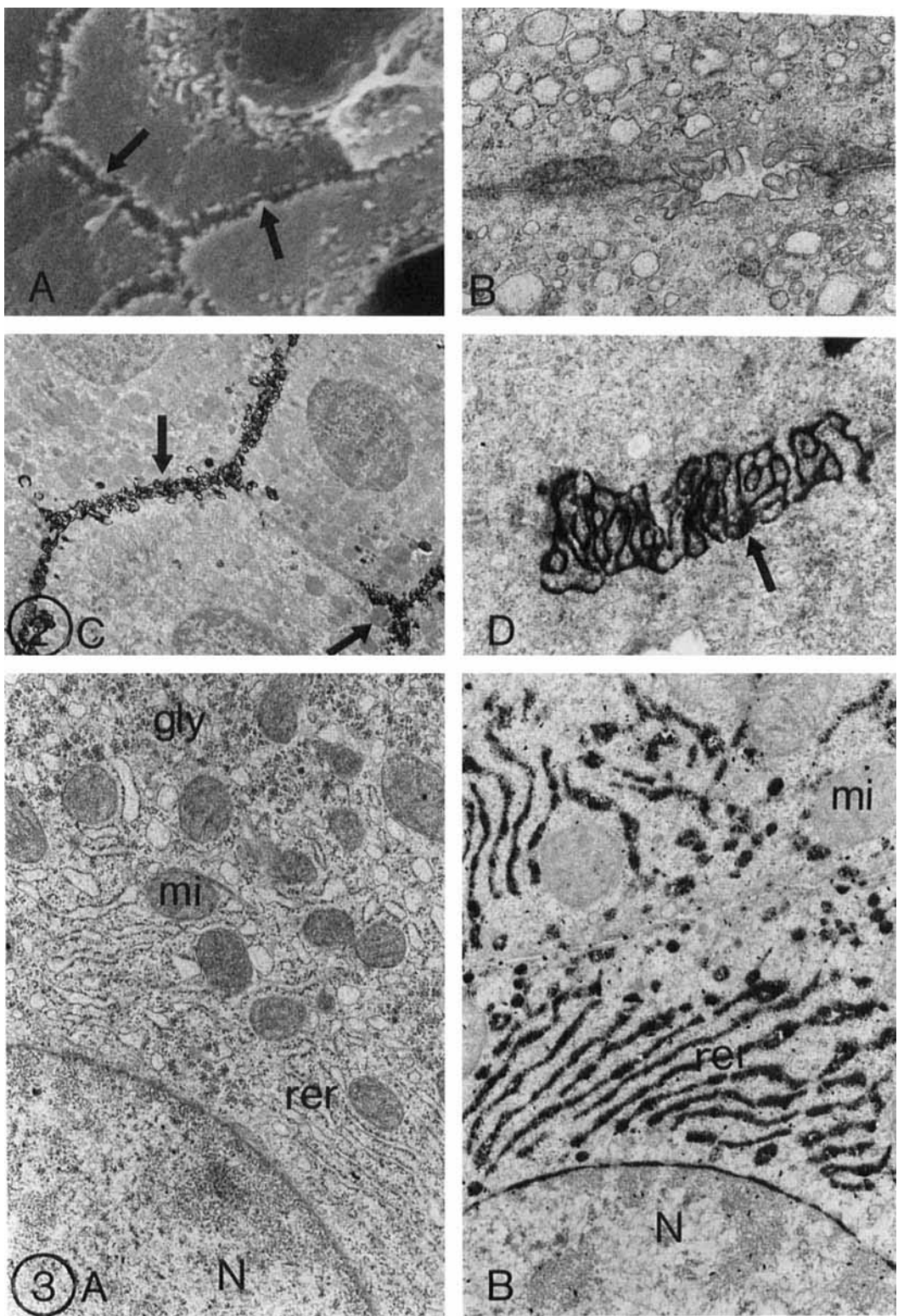


Fig. 2. Normal liver. **A:** Scanning electron micrograph of bile canalicular network (arrow). **B:** Bile canalculus with microvilli, tight junctions, and desmosomes. **C,D:** Strong adenosine triphosphatase activity is present at the canalicular surface of hepatocytes (arrow). **A:** $\times 3,000$; **B:** $\times 13,400$; **C:** $\times 3,000$; **D:** $\times 13,400$.

Fig. 3. Normal liver. Note nucleus (N), prominence of rough endoplasmic reticulum (rer), numerous mitochondria (mi), and glycogen particles (gly). **A:** Uranyl acetate, lead citrate stain. **B:** Positive glucose-6-phosphatase reaction in the endoplasmic reticulum (rer) and in the nuclear envelope. **A:** $\times 13,400$; **B:** $\times 12,000$.

provided with a double membrane (Figs. 1B, 3A). Changes in size and form of cristae of the mitochondria are an early, but unspecific, indication of cellular injury. The stored glycogen appears in two forms: as monoparticulate (beta) granules and as aggregates arranged in rosettes (alpha particles) (Figs. 1B, 3A). The cytoskeleton, which includes microfilaments (4–7 nm), intermediate filaments (11 nm), and microtubules (120–26 nm), regulates cell shape, secretion, and division (Denk and Franke, '82). Toxic chemicals, alcohol, and drugs greatly alter cytoskeletal function, and the injury caused by them can be observed, for example, as Mallory bodies.

VIRAL HEPATITIS

The morphological features of acute viral hepatitis are well known and are characterized by a combination of hepatocellular injury, proliferation, and inflammation (Bianchi, '70; Ishak, '73; Popper, '75; Schaff et al., '86c; Scheuer, '87; Simson and Gear, '87; Zuckerman, '84; Lapis and Schaff, '79). Ballooning degeneration is a common feature in acute hepatitis and results from the dilated, vesicular endoplasmic reticulum (Fig. 4A). Ballooning is believed to be associated with changes in ion and water regulation within the cell (Trump et al., '76). Autophagic vacuoles are prominent, and the appearance of bile pigment in the hepatocytes is frequent (Figs. 4C, 5A, 5C). Acidophilic degeneration, necrosis, and Councilman-like bodies are the signs of coagulative necrosis of hepatocytes. The dehydrated, small, round, sharply defined bodies, lying free among other hepatocytes, contain shrunken organelles and, occasionally, portions of clumped nuclei (Fig. 4B).

Roundish, lamellar bodies occur often, especially in non-A, non-B hepatitis (Figs. 5A, 5C). These inclusions are believed to be phospholipid bilayers formed by the interaction of bile with membrane phospholipids (Lapis and Schaff, '79; Trump et al., '76). The Golgi complex is usually extended and packed with a large number of lipoprotein particles measuring 50–60 nm in diameter in cases of post-transfusion non-A, non-B hepatitis (Fig. 5B). The lamellar bodies are similar to the tubular changes seen in the hepatocytes of chimpanzees infected with a human agent of non-A, non-B hepatitis (Jackson et al., '79; Schaff et al., '84; Shimuzu et al., '79; Figs. 6A–D). However, the membranous inclusions in the liver of infected chimpanzees are connected with membranes of the endoplasmic reticulum (Figs. 6A–C), and they consist of two parts: a unit membrane and an amorphous part with a 16-nm periodicity (Fig. 6D) (Schaff et al., '85). Cytochemical analysis of these inclusions found them similar to the syringe-shape inclusions observed in the lymphoid cells of patients with acquired immunodeficiency syndrome (AIDS) (Kostianovszky et al., '87).

Alterations of nuclei and nucleoli are frequent and include the formation of pseudoinclusions, enlargement, and fragmentation of nucleoli, and an increased number of nuclear bodies (Lapis and Schaff, '79). Aggregates of 22–25-nm nuclear particles, which have been suggested as a marker for experimental and human non-A, non-B hepatitis (Shimizu et al., '79), were found in every type of human hepatitis and in

chimpanzees before inoculation with infectious material (Schaff et al., '84, '85). Therefore, these aggregates are not specific for non-A, non-B hepatitis.

The isolated viral particles causing viral hepatitis, such as hepatitis B virus (HBV), can be easily recognized by negative staining (Fig. 7A). The surface antigen of the HBV (HB_sAg) may accumulate in the cytoplasm of hepatocytes, referred to as "ground-glass hepatocytes" by light microscopy (Fig. 7C) and can be demonstrated by immunohistochemical methods (Fig. 7B). Ultrastructurally, the tubules of HB_sAg measure 22 nm in diameter and are located in the cisternae of the endoplasmic reticulum (Figs. 7D, 7E). The hepatitis B core particles can be identified in the nuclei of infected hepatocytes as rings measuring 27 nm in diameter (Fig. 7F).

Different types of ultrastructural changes have been thought to be virus-related structures in non-A, non-B hepatitis (Iwarson et al., '85). However, none of these were found to correspond to the non-A, non-B agent itself, which remains unidentified.

In chronic active hepatitis a close interaction between hepatocytes and lymphocytes, accompanied by deposition of collagen fibers in the Disse and intercellular spaces, can be observed (Figs. 8A, 8B). Different degrees of necrobiotic changes occur, especially in the periportal area, and correspond to "piecemeal" necrosis observed by light microscopy. The tubular membrane alterations are thought to be markers for non-A, non-B hepatitis in chimpanzees. The tubuloreticular inclusions (Schaff et al., '82) were observed after recombinant alpha-interferon (IFN) treatment of patients with HBV-positive chronic active hepatitis (Figs. 9A–C) (Schaff et al., '86a). Ultrastructural studies did not facilitate our understanding of the mechanism responsible for chronicity of acute hepatitis, but they did explain the morphological features seen by light microscopy at the subcellular level.

INJURY BY DRUGS AND TOXINS

The significance of drug and toxin-induced liver damage has increased in the last two decades and has been reviewed in several recent reports (Ishak, '82; Phillips et al., '87; Wilson, '86; Zimmerman and Ishak, '87). The intrinsic and idiosyncratic hepatotoxins can reproduce the entire spectrum of liver diseases (Zimmerman and Ishak, '87). Opinions concerning the value of electron microscopy in assessing toxin-induced liver diseases are divergent (Jezequel and Orlandi, '72; Phillips et al., '87; Schaff and Lapis, '79b; Tanikawa, '79; Zimmerman and Ishak, '87).

Adaptive changes in the form of ground-glass hepatocytes (Fig. 10A) are common features seen after taking drugs that are metabolized in the smooth endoplasmic reticulum (ser). The expressed proliferation of ser is very characteristic at the ultrastructural level, for example, after treatment with phenothiazine (Fig. 10D), oral contraceptives (Fig. 10B), and rifampicin (Fig. 10C). Dilatation of the rer caused by oxyphenacetin and several other drugs appears as ballooned hepatocytes at the light microscopic level (Fig. 10E).

Variations in the size and number of mitochondria, as well as their pleomorphism, occur after treatment

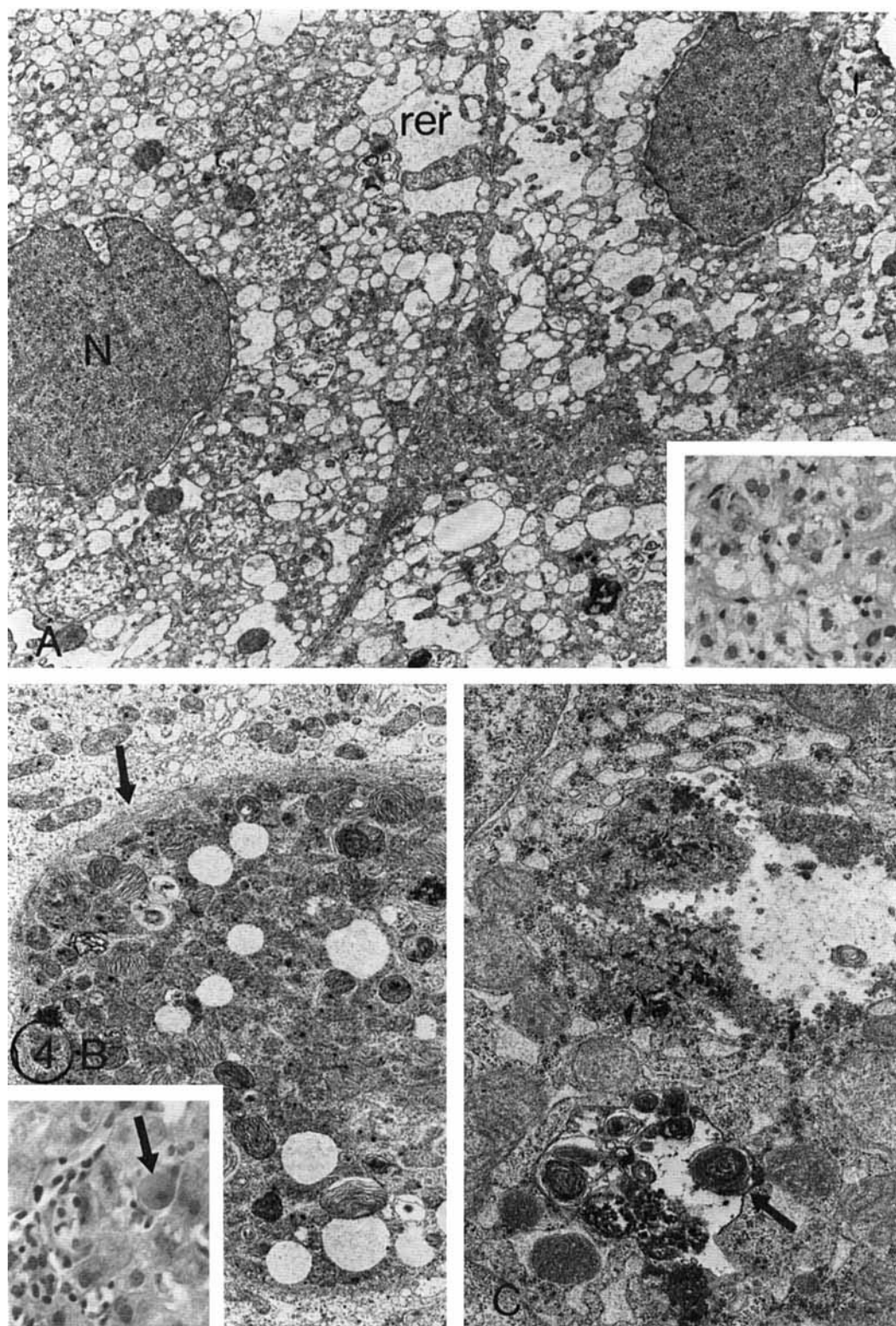


Fig. 4. Acute viral hepatitis. **A:** Balloon hepatocytes with dilation of rough endoplasmic reticulum (rer) and nucleus (N). **Inset:** balloon cells by light microscopy. **B:** Councilman-like body (arrow) by electron

microscopy. **Inset:** by light microscopy (arrow). **C:** Focal cytoplasmic degeneration and necrosis (arrow). **A:** $\times 10,000$, **inset:** $\times 150$, **B:** $\times 8,400$; **inset:** $\times 150$; **C:** $\times 13,200$.

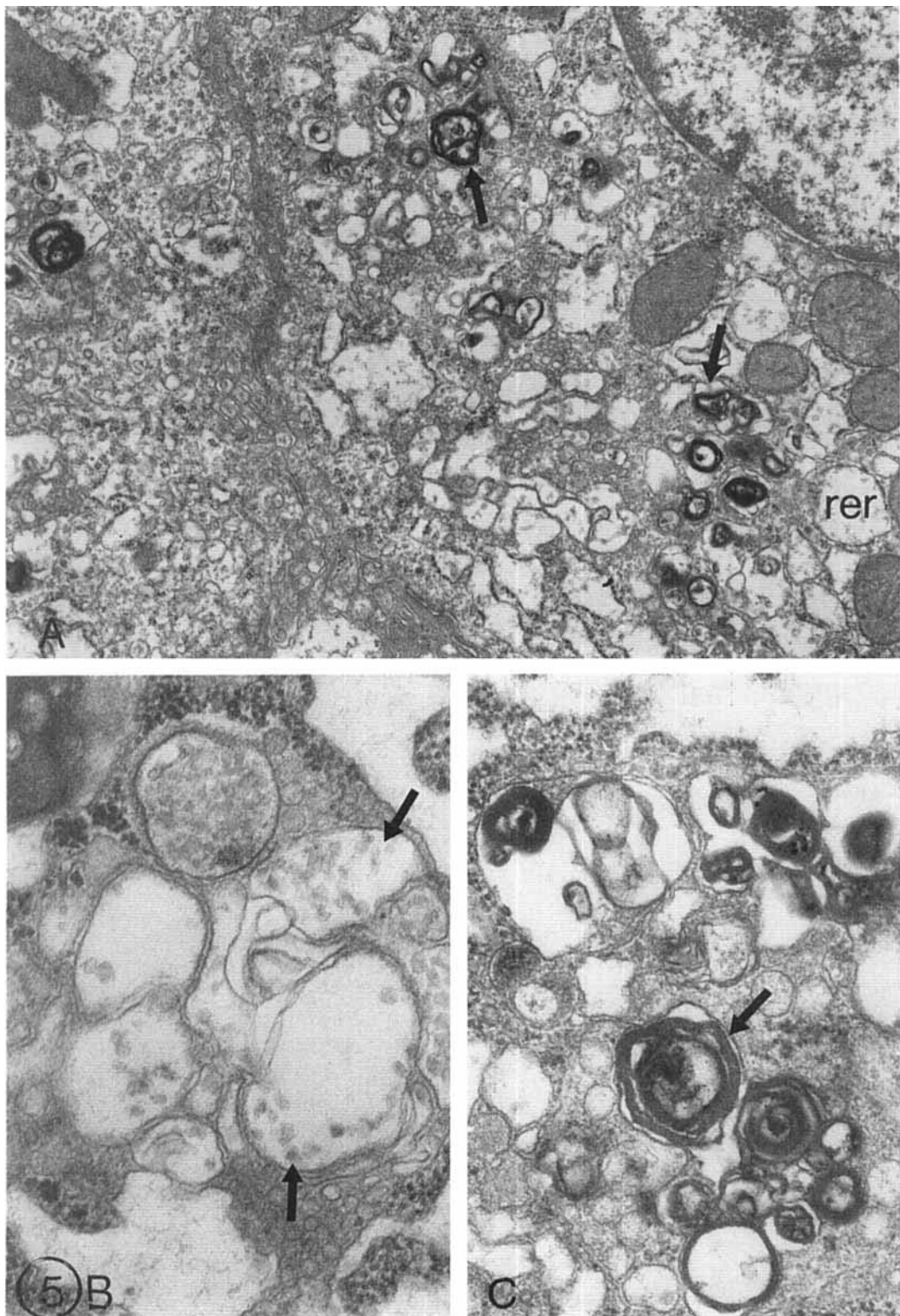


Fig. 5. Acute non-A, non-B hepatitis. **A:** Dilation of rough endoplasmic reticulum (rer); large number of cytolysosomes (arrows). **B:** Lipoproteins (arrows) accumulate in the distended Golgi complex. **C:** Dense, lamellated bodies are numerous (arrow). **A:** $\times 19,200$; **B:** $\times 72,000$; **C:** $\times 36,000$.

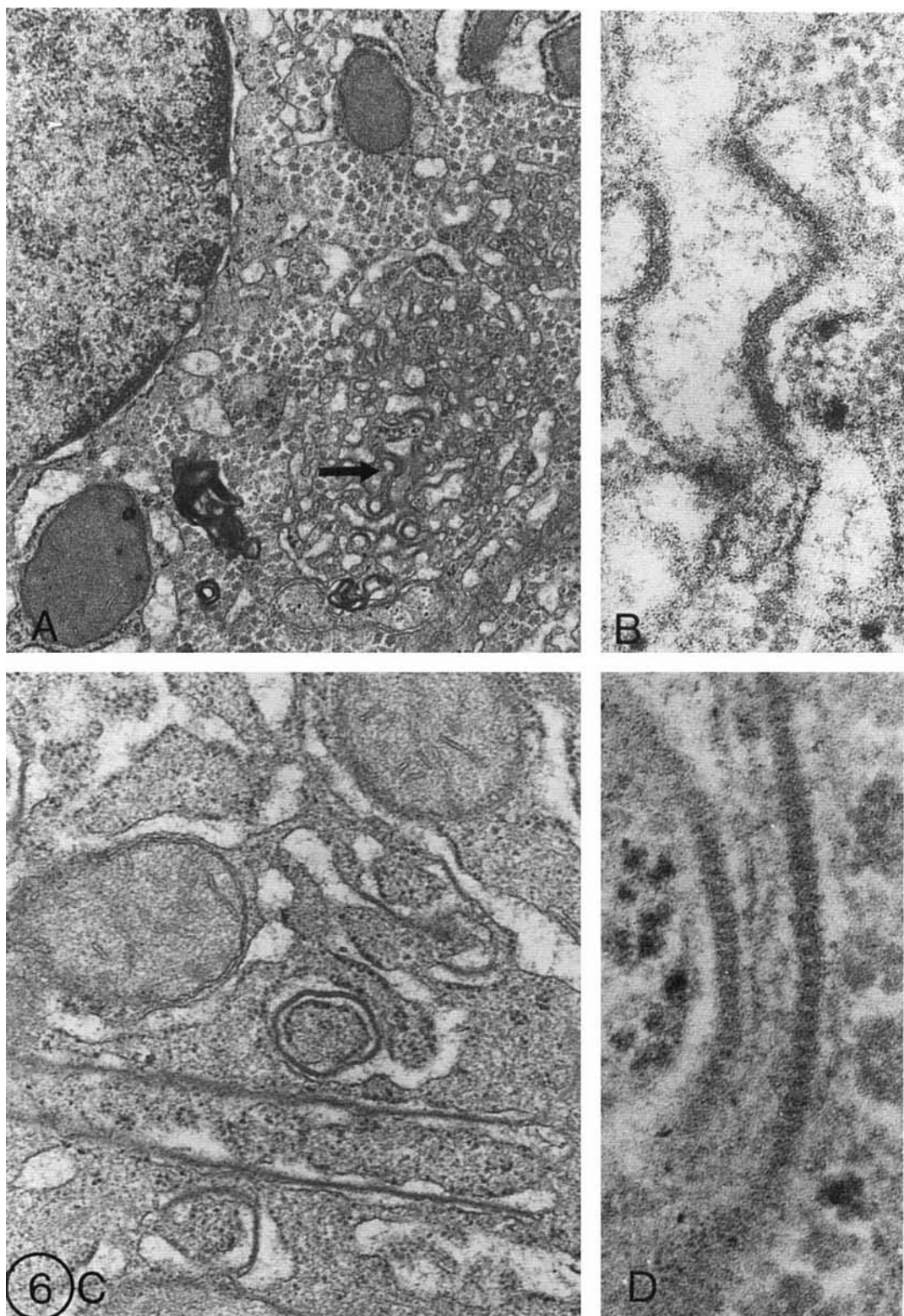


Fig. 6. Non-A, non-B hepatitis-infected chimpanzee liver. **A:** Proliferation of endoplasmic reticulum membranes (arrow). **B:** The latter are composed of a unit membrane and an amorphous material. **C:** Cylindrical and ring-shaped inclusions are connected with the endoplasmic reticulum. **D:** Periodicity (16-nm) in the wall of the inclusions. **A:** $\times 24,000$; **B:** $\times 120,000$; **C:** $\times 36,000$; **D:** $\times 120,000$.

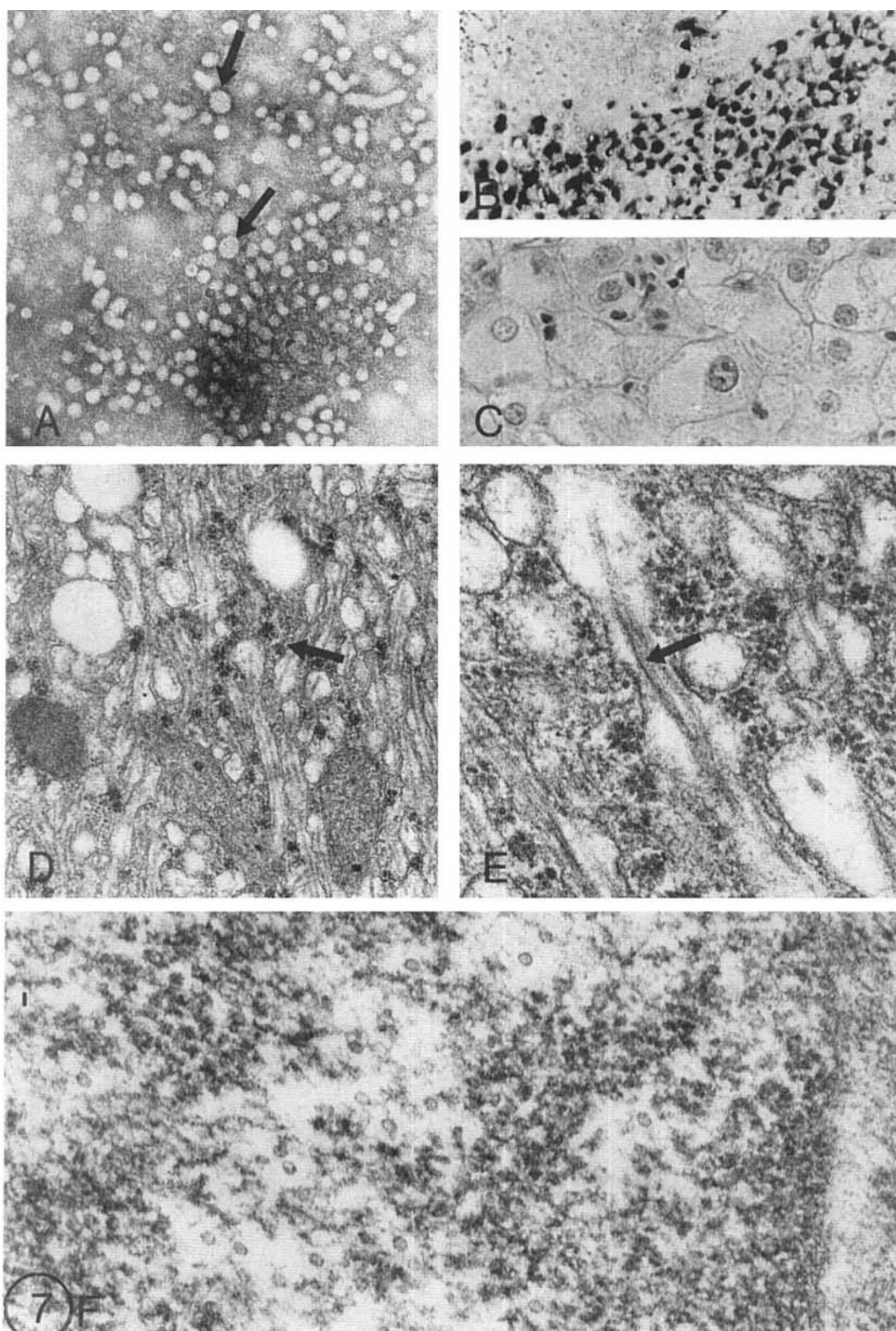


Fig. 7. Hepatitis B virus (HBV). **A:** Negative staining with phosphotungstic acid. Tubules and spherules (22 nm in diameter) and also Dane particles (42 nm in diameter; arrow) can be observed. **B:** HB_sAg with avidin-biotin complex immunohistochemical staining. **C:**

Ground-glass hepatocytes in a carrier's liver. **D,E:** Filamentous component of HB_sAg in dilated endoplasmic reticulum (arrow) **F:** Core particles in the karyoplasm of a HBV-infected hepatocyte. **A:** $\times 90,000$; **B:** $\times 150$; **C:** $\times 400$; **D:** $\times 12,000$; **E:** $\times 99,000$; **F:** $\times 66,000$.

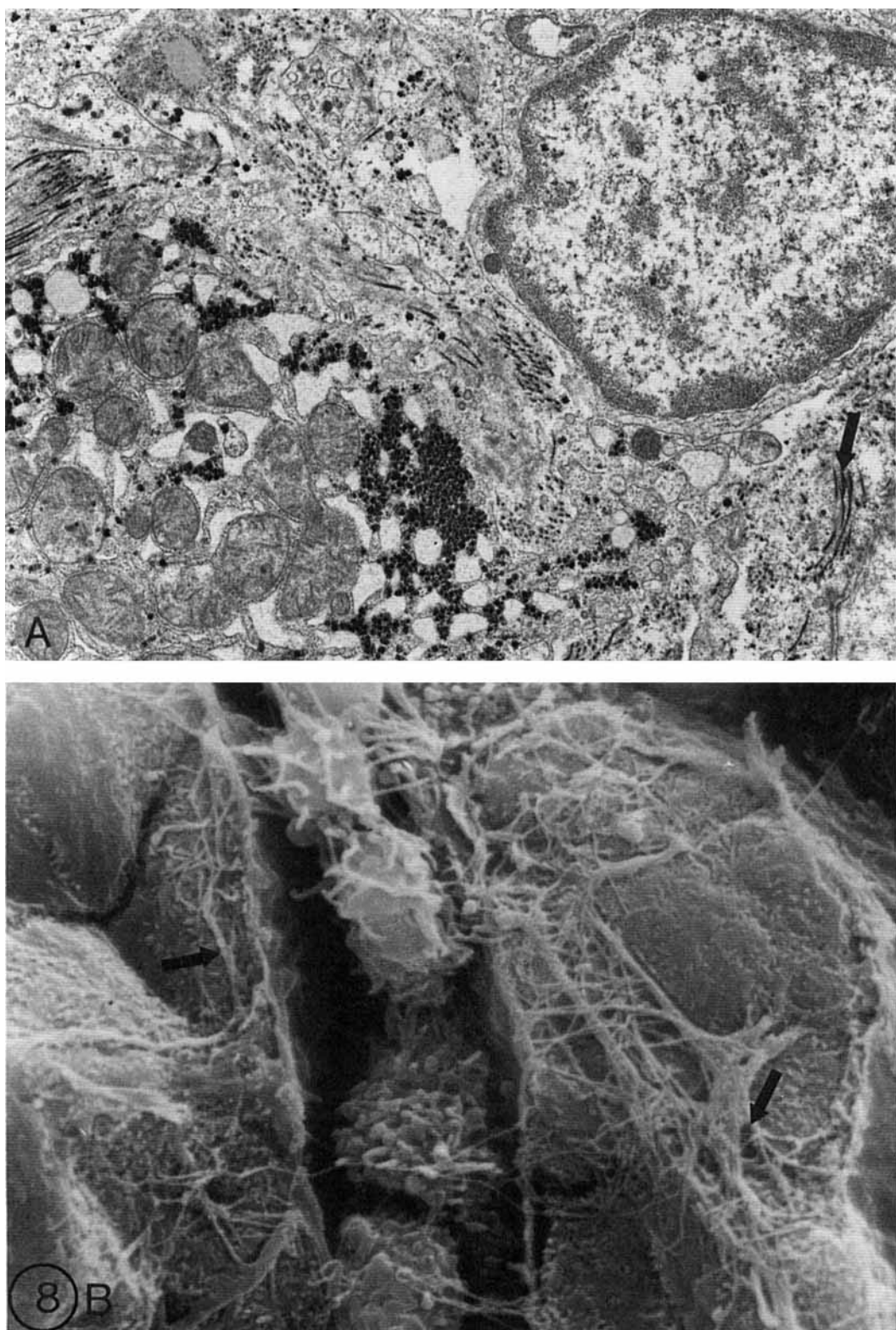


Fig. 8. Chronic active hepatitis. **A:** Chronic inflammatory cells are in close contact with the hepatocytes and fill the dilated sinusoids (arrow). **B:** Collagen fibers appear around the hepatocytes (arrows). **A:** $\times 9,600$; **B:** $\times 6,000$.

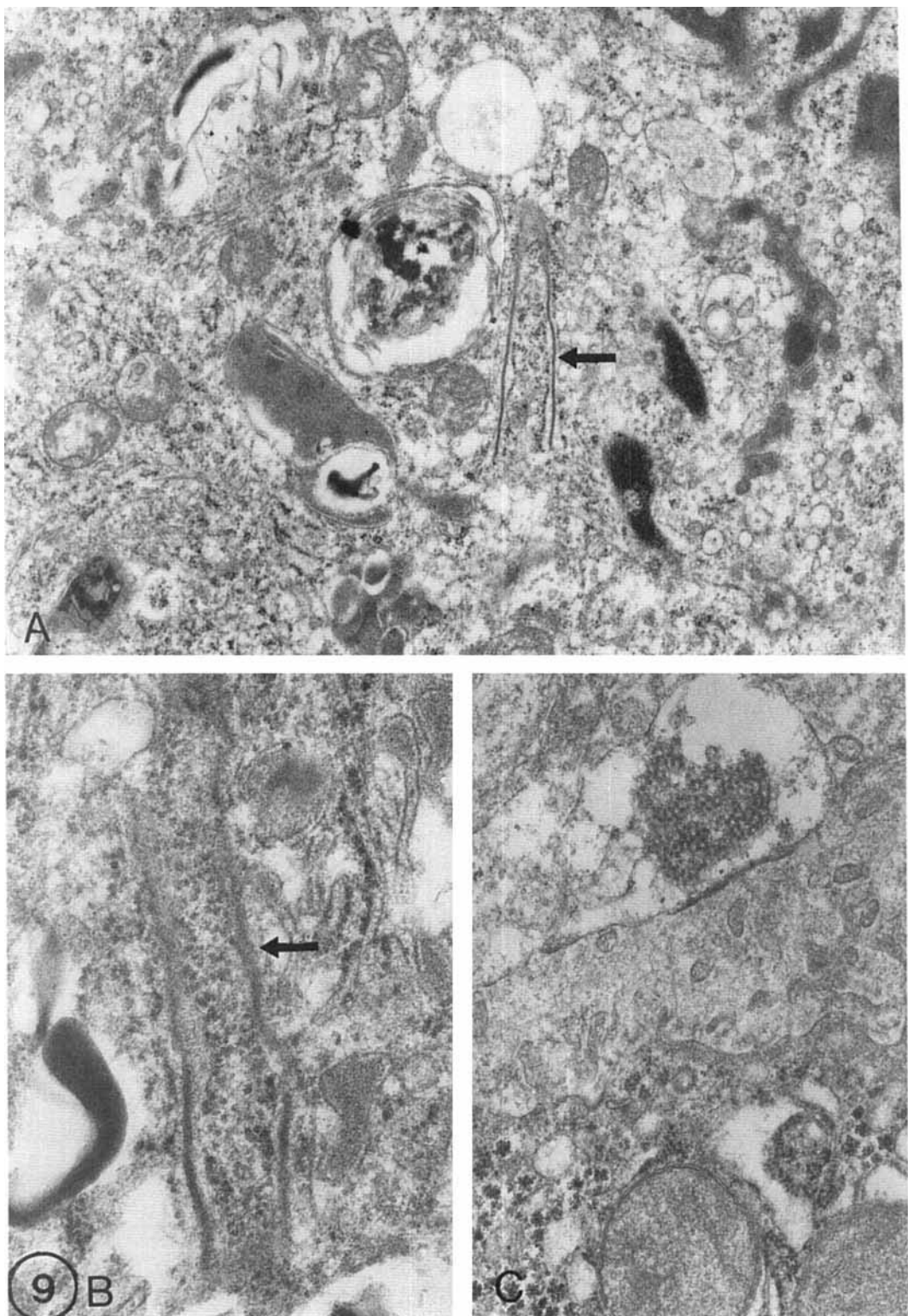


Fig. 9. Chronic active hepatitis after treatment with human alpha-interferon. **A,B:** Syringe-shape inclusions (arrow) in macro-

phages. **C:** Tubuloreticular inclusion in an endothelial cell. **A:** $\times 16,000$; **B:** $\times 33,000$; **C:** $\times 30,000$.

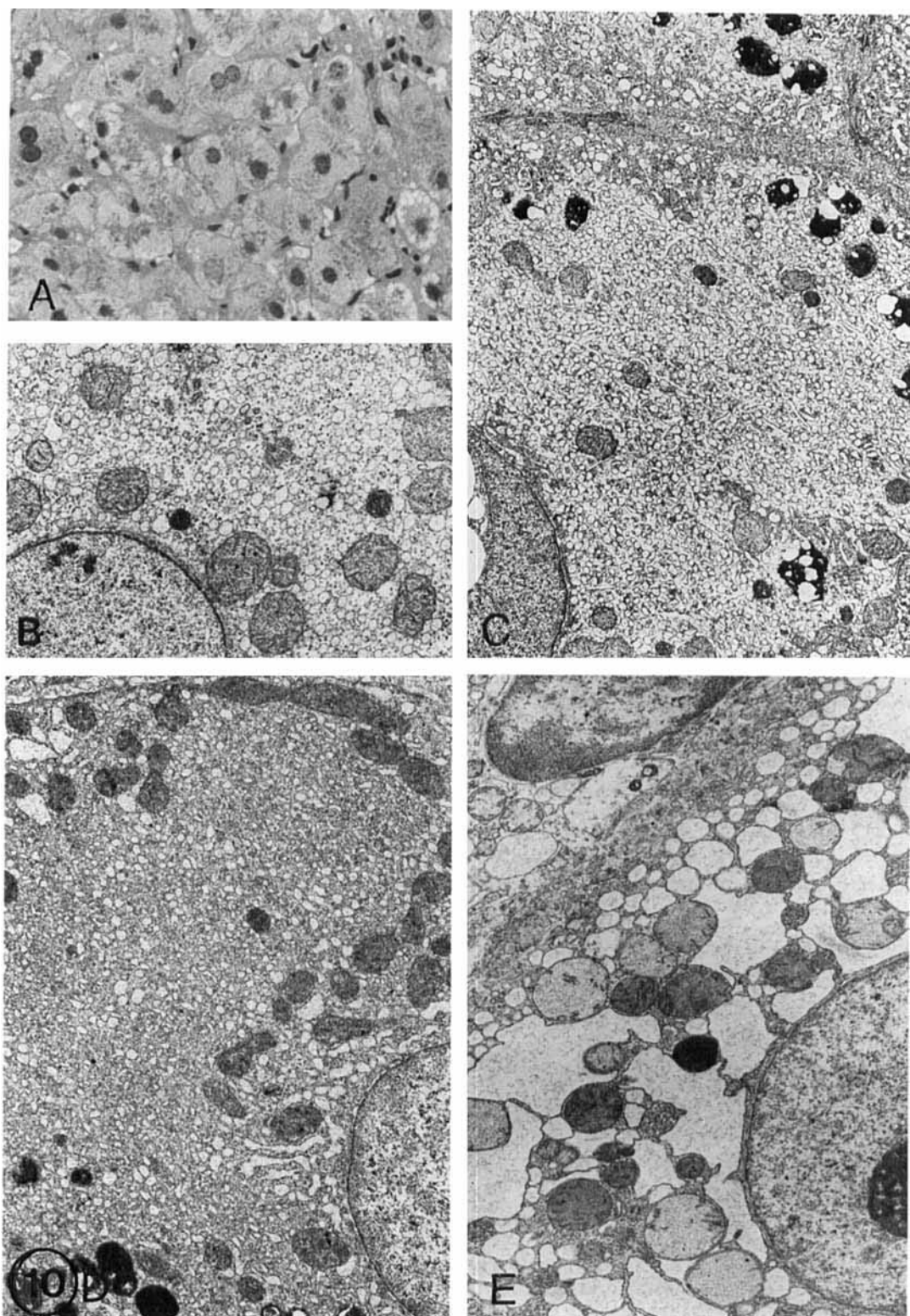


Fig. 10. Drug-induced liver alterations. **A:** Ground-glass hepatocytes and balloon cells. Decrease of rough endoplasmic reticulum and proliferation of smooth endoplasmic after **B:** oral contraceptive, **C:** rifampicin, and **D:** phenothiazine treatment. **E:** Marked dilation of endoplasmic reticulum after oxypheniacetin treatment. **A:** $\times 250$; **B:** $\times 8,000$; **C:** $\times 7,000$; **D:** $\times 7,000$; **E:** $\times 12,000$.

with several drugs, such as chloramphenicol and analgesics (Phillips et al., '87; Schaff and Lapis, '79b). Giant mitochondria containing paracrystalline inclusions are especially common after taking oral contraceptives (Fig. 11A) and drugs causing cholestasis. Macrovesicular and microvesicular forms of steatosis are frequently observed after the administration of a large variety of drugs (Fig. 11B). An increase in the number of lysosomes, cytolyticosomes, and lipofuscin granules may follow the exposure to several chemicals (Figs. 11C-E).

The cholestatic injury caused by drugs is indistinguishable from other forms of cholestasis on the basis of electron microscopy. Dilation of bile canaliculi, loss of microvilli, bleb formation, thickening of pericanalicular ectoplasm (Fig. 11F), and bile pigment deposits are all signs of arrested bile flow. Based on ultrastructural alterations, Phillips et al. ('87) classified the drug- and toxin-induced hepatic changes into major and minor categories. They assumed, in accordance with our opinion, that drug and toxic effects are not "entirely non-specific." A combination of "major" and "minor" ultrastructural changes may be characteristic for certain drug effects. These combinations might illustrate the primary target organelle involved in the metabolism or the primary site of the injury caused by the drug in question.

ALCOHOLIC LIVER DISEASE

Alcoholic liver disease is the most common and well known form of toxic liver injury, whose spectrum includes fatty liver, alcoholic hepatitis, and cirrhosis (Galambos, '85; Hall, '87; MacSween and Burt, '86; Popper et al., '81). The fatty change in micro- or macrovesicular forms is the most common alteration (Fig. 12A). However, the most specific morphological change seen in alcoholic hepatitis is the appearance of alcoholic hyaline or Mallory bodies. These bodies are composed of two subtypes of cytokeratins that form a conglomerate of branching filaments (Figs. 12A inset, 12B, 12C). The fibrils subsequently condense to an electron-dense homogenous mass (Fig. 12C; Franke et al., '79). Paracrystalline inclusions living free in the cytoplasm often occur in the alcoholic liver (Fig. 12D, Schaff and Lapis, '79). Variations in the size and appearance of paracrystalline inclusions in the mitochondria are a common early sign of alcoholic liver disease (Fig. 12E). Early stages of perisinusoidal fibrosis ("capillarization" of the sinusoid) also can be detected by electron microscopy (Phillips et al., '87; Schaff and Lapis, '79).

CHOLESTASIS

Cholestasis means the reduction or arrest of bile flow. Morphologically, cholestasis corresponds to a visible accumulation of bile pigment (Desmet, '87). Electron microscopy is a highly sensitive tool for revealing cholestasis, since it visualizes changes even before they are detected by light microscopy (Desmet, '87; Phillips et al., '87). The essential phenomena of cholestasis are those changes that occur in the "bile secretory apparatus" of hepatocytes (Popper and Schaffner, '63; Schaff and Lapis, '79a). Desmet ('87) has

pointed out that the complete "hepatocellular machinery" is involved in bile production, which includes the uptake, transport, conjugation, and secretion of bilirubin.

The most conspicuous alterations found in cholestasis are the changes in the bile canalculus. The normal, finger-like microvilli (Fig. 13A) disappear (Fig. 13B) from the ectatic canalicular surface, and bleb formation often occurs (Fig. 13C). Pericanalicular ectoplasmic thickening and the disappearance of the contractile microfilamentous meshwork may be noted (Fig. 13B). The dilated canalicular lumen may be empty, partially filled (Fig. 13B), or completely filled with bile plugs (Fig. 13D). These canalicular changes may be attributed to an increase in intraluminal pressure or the "paralytic ileus" of the cytoskeletal contractile system (Desmet, '87). The bile pigment that accumulates in the canalicular and hepatocytes is either granular or fibrillar in appearance (Fig. 13E). The irregular lamellar structures probably correspond to the liquid-crystalline phase of conjugated bile salts, phospholipids, and cholesterol (Fig. 13E).

Secondary phenomena associated with cholestasis include lobular, portal, and periportal reactions. Although certain cholestatic liver diseases exhibit distinctive ultrastructural features, the distinction between intra- and extrahepatic types of cholestasis is not possible, based solely on ultrastructural parameters (Phillips et al., '87; Schaff and Lapis, '79a).

METABOLIC LIVER DISORDERS

Ultrastructural analysis of liver biopsy specimens taken from patients with metabolic disease is important in establishing the diagnosis. The accumulation of a metabolite resulting from a defective enzyme appears in a highly specific, characteristic, and visible form in hepatocytes and cells of mesenchymal origin in a wide spectrum of metabolic disorders. In some cases the light microscopic examination of the liver only raises suspicion, whereas the ultrastructural observations establish the diagnosis. Secondary changes resulting from metabolic alterations, for example, fibrosis or fatty liver, often complicate the basic, primary disorder (Ishak and Sharp, '87; Knight and Wu, '82; Phillips et al., '87). A brief survey of the most important and common alterations follows.

Disorders of carbohydrate metabolism, including several forms of glycogen storage diseases (galactosemia, hereditary fructose intolerance, and diabetes mellitus), are characterized by abnormal forms and an excess accumulation of glycogen. For example, monoparticulate nuclear glycogenogenesis occurs in diabetes mellitus and in Gierke's disease, that is, type I glycogen storage disease (Fig. 14A). The "starry-sky" pattern of glycogen particles and the formation of glycogen inclusions have been described in different types of glycogen storage diseases (Phillips et al., '87). Large lipid droplets and extensive vesicularization of endoplasmic reticulum can be seen in galactosemia (Fig. 14B).

Several types of lysosomal storage diseases are almost pathognomonic at the ultrastructural level. In Gaucher's disease, tubular inclusions containing glucocere-

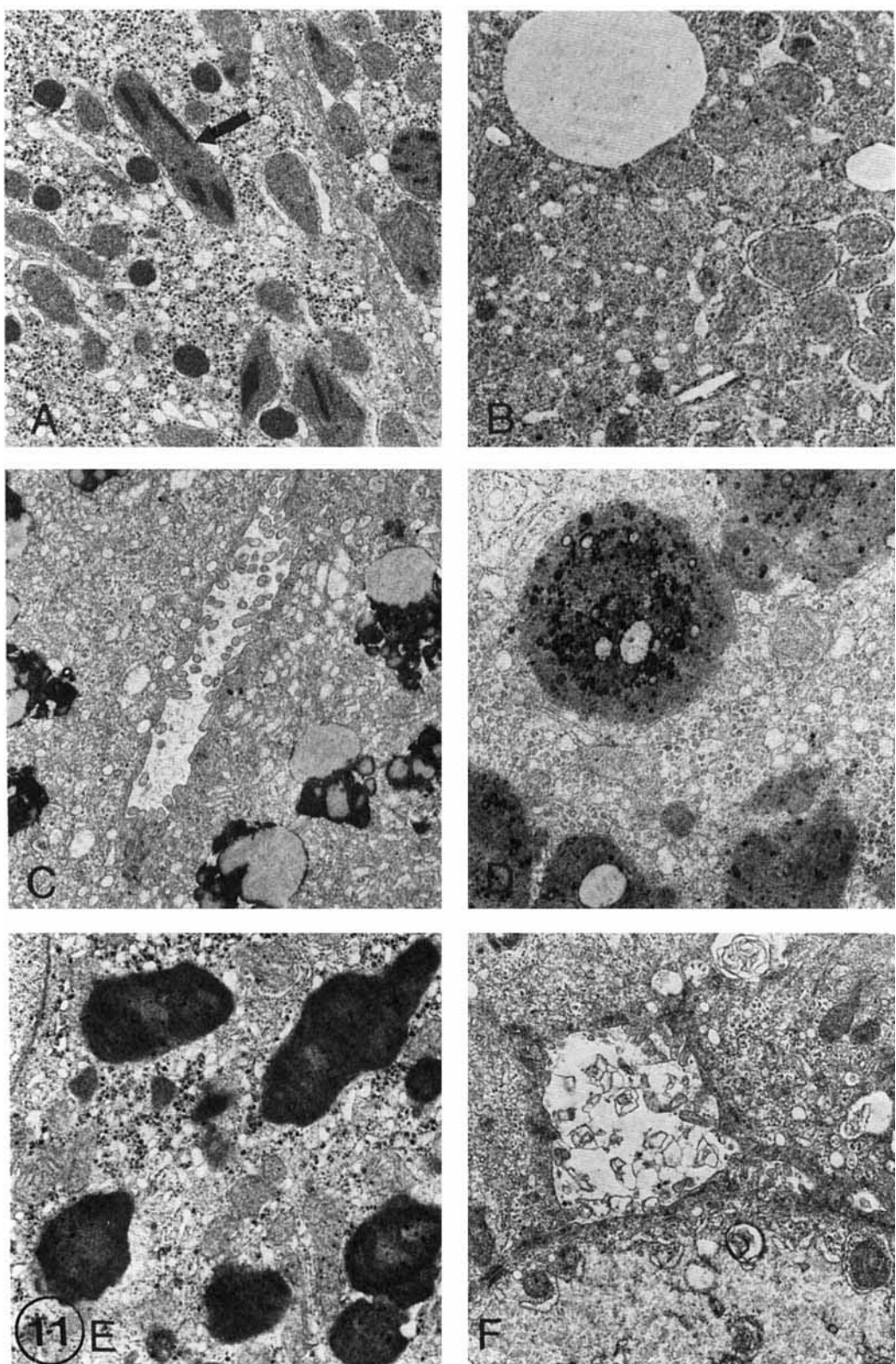


Fig. 11. Drug and toxic effect. **A:** Variation in size and shape of mitochondria containing paracrystalline inclusions (arrow). **B:** Lipid droplets; **C:** large lipofuscin granules; **D:** lipolysosomes; **E:** enlarged lysosomes after acetaminophen overdose; **F:** intracanalicular and cytoplasmic cholestasis after oral contraceptives. **A:** $\times 6,000$; **B:** $\times 10,000$; **C:** $\times 12,000$; **D:** $\times 6,600$; **E:** $\times 6,600$; **F:** $\times 8,000$.

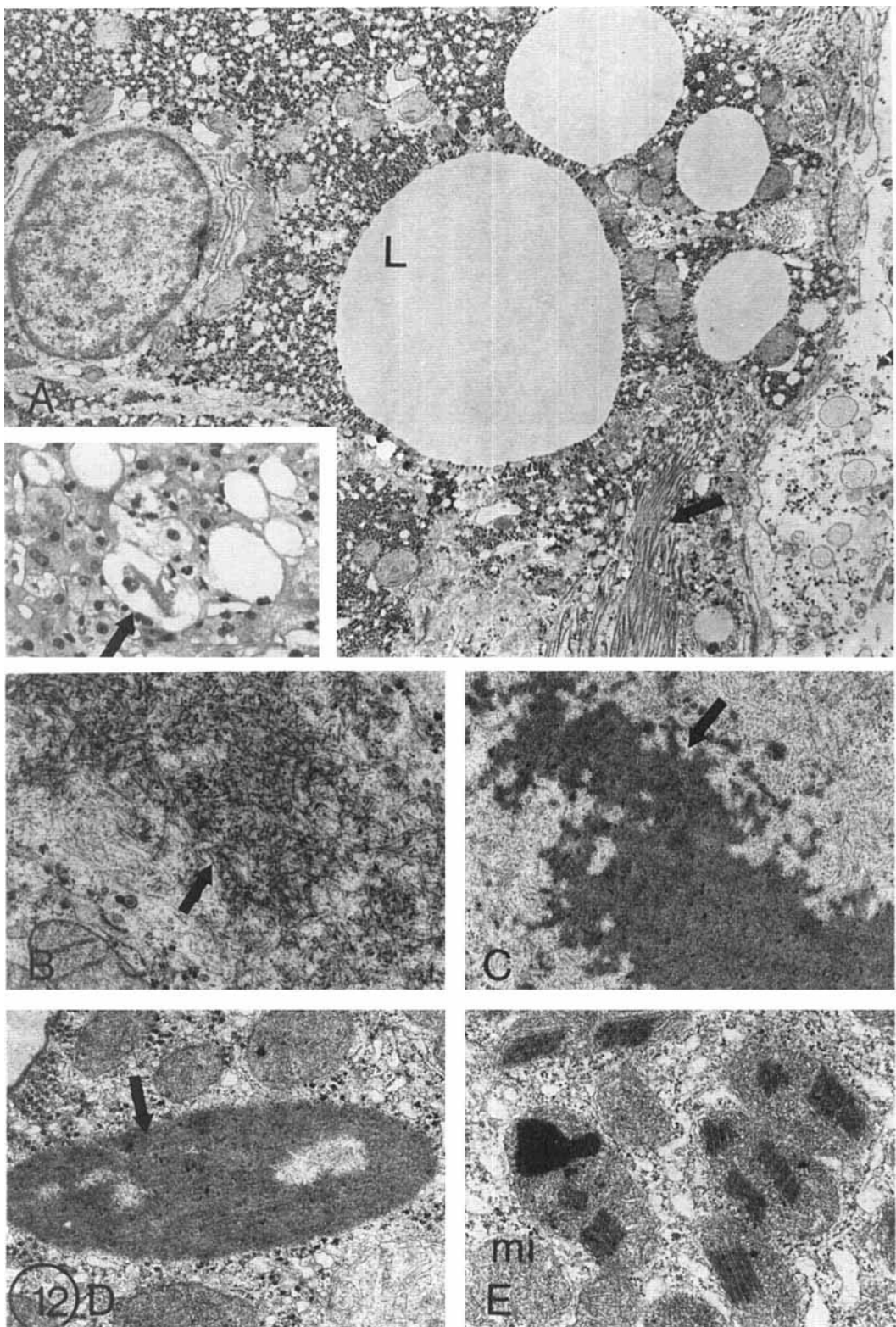


Fig. 12. Alcoholic liver disease. **A:** Large lipid droplets (L); collagen fibers (arrow) along the sinusoids. **Inset:** Balloon hepatocyte containing alcoholic hyaline (arrow). **B:** Fibrillary form (arrow) and **C:** condensed form (arrow) of alcoholic hyaline. **D:** Crystalline inclu-

sion lying free in the cytoplasm. **E:** Mitochondria containing inclusions. **A:** $\times 5,000$; **Inset:** $\times 150$; **B:** $\times 17,000$; **C:** $\times 17,000$; **D:** $\times 13,400$; **E:** $\times 16,500$.

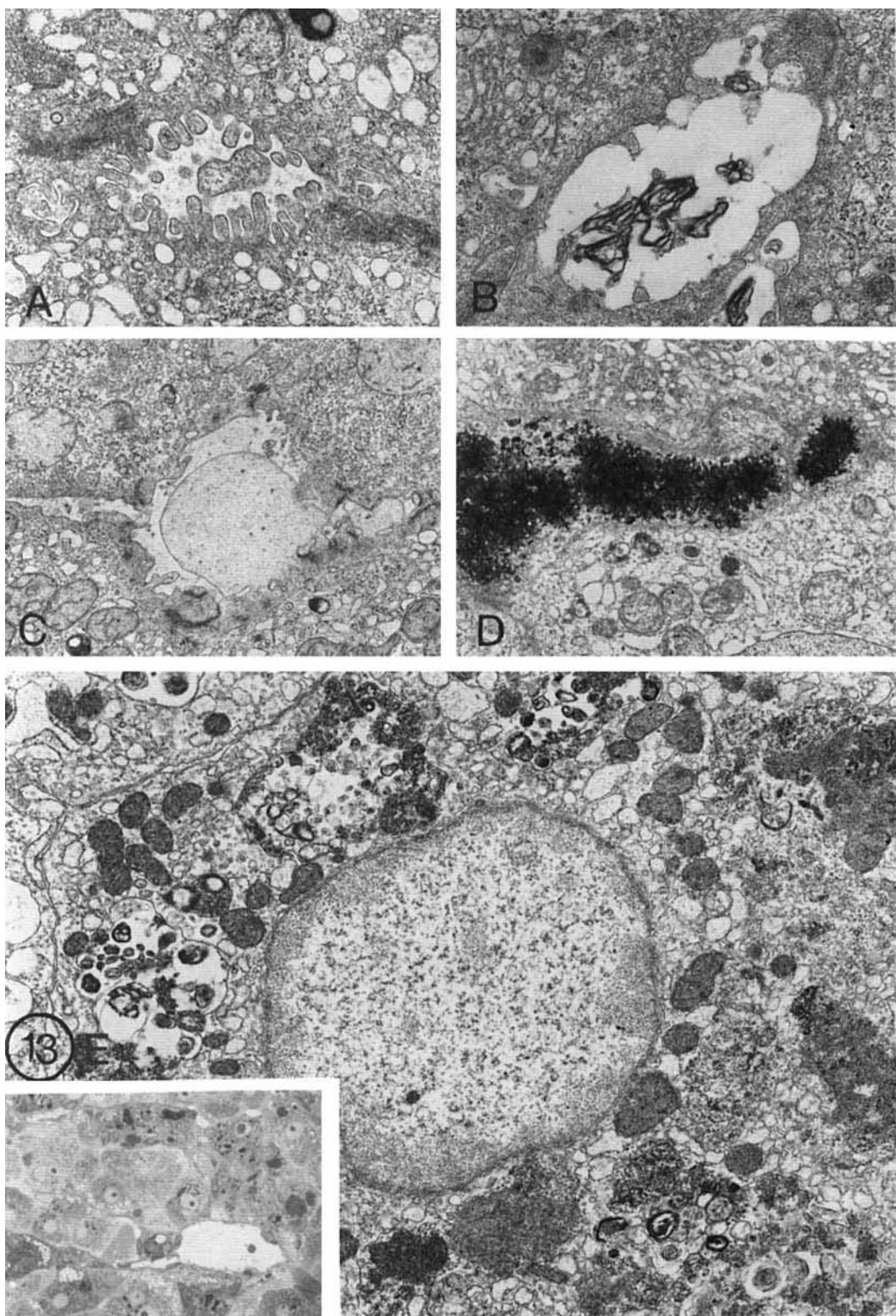


Fig. 13. Cholestasis. **A:** Normal bile canalculus; **B:** dilated bile canalculus containing lamellar bile material; **C:** bleb formation; **D:** bile plug extends the canalculus; **E:** intracytoplasmic cholestasis. **Inset:** centrolobular cholestasis. **A:** $\times 13,400$; **B:** $\times 16,600$; **C:** $\times 8,000$; **D:** $\times 8,000$; **E:** $\times 12,500$; **Inset:** $\times 250$.

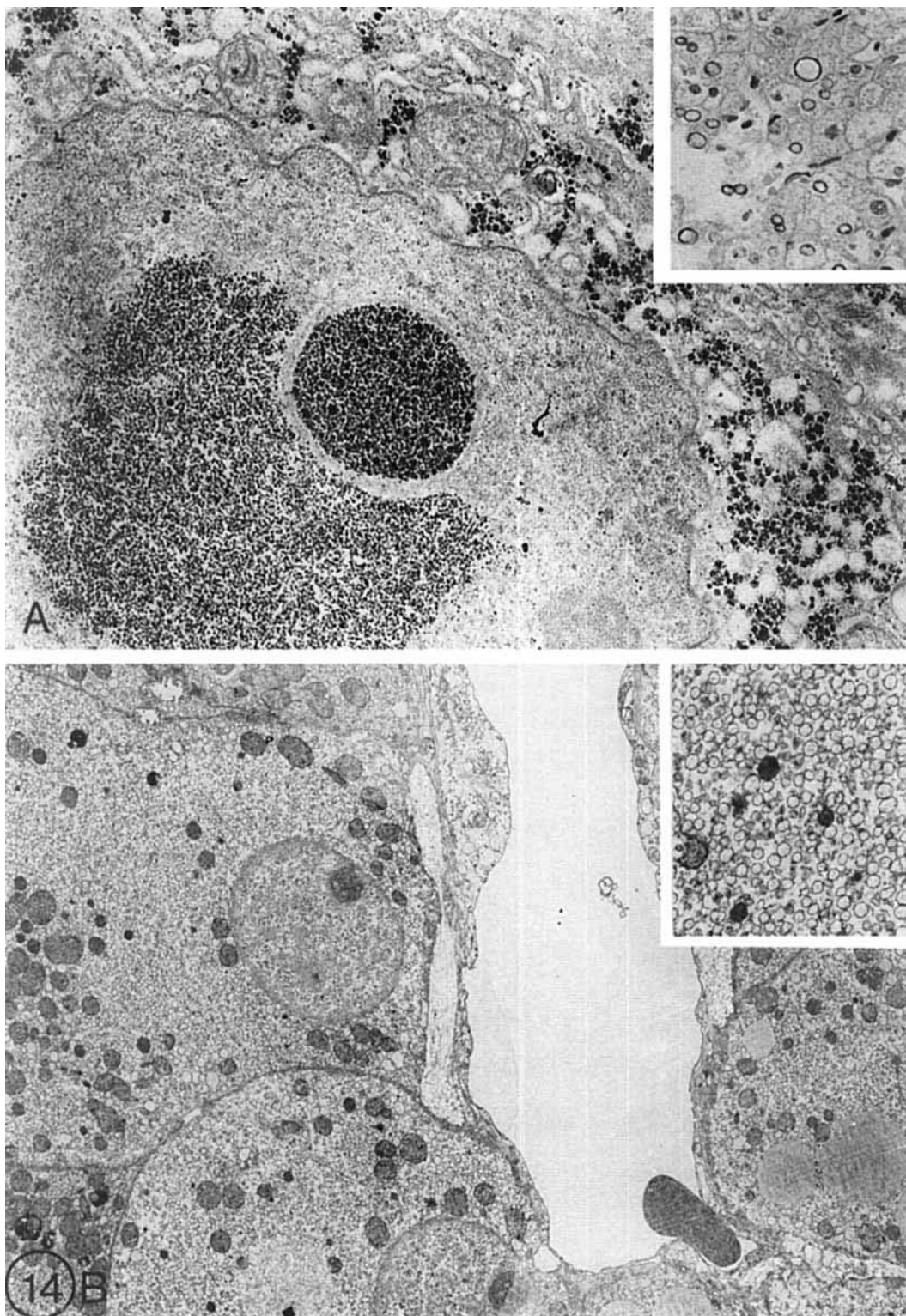


Fig. 14. Metabolic disease. **A:** Intranuclear monoparticulate glycogen particles in diabetes mellitus by silver proteinate staining. **B:** Increase of smooth endoplasmic reticulum (ser) and lipid (L) droplets. **Inset:** higher magnification. **A:** $\times 12,500$, **Inset:** $\times 200$; **B:** $\times 6,000$, **Inset:** $\times 10,000$.

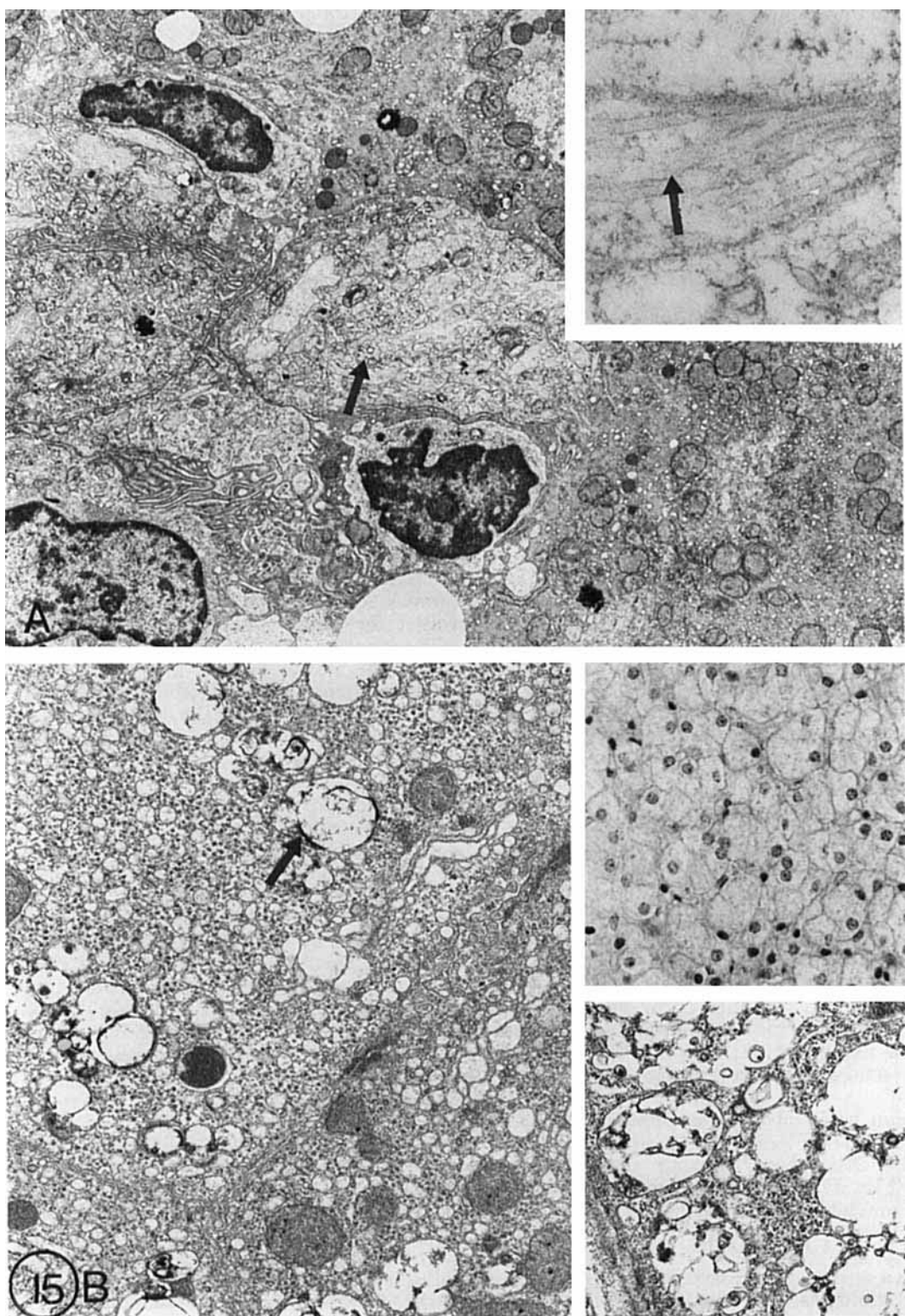


Fig. 15. Metabolic diseases. A: Gaucher's disease. Tubular inclusions (arrow) in macrophages; degenerative changes in hepatocytes. Inset: structure of a tubular inclusion at higher magnification (arrow). B: Niemann-Pick disease; myelin-like lamellated inclusions

in the hepatocytes (arrow). Inset top: the hepatocytes have a foamy appearance by light microscopy. Inset bottom: the inclusions at higher magnification. A: $\times 5,000$, Inset: $\times 50,000$; B: $\times 12,500$, Inset top: $\times 200$, Inset bottom: $\times 16,500$.

broside occur in the Kupffer cells (Fig. 15A; Lapis, '79b; Peters et al., '77). The number of lysosomes increases in the hepatocytes, but no tubular inclusions appear. In sphingomyelin lipidosis or Niemann-Pick disease, concentrically laminated, myelin-like formations appear as membrane-bound inclusions in the hepatocytes (Fig. 15B) and Kupffer cells. Numerous with enlarged lysosomal inclusions localize in the liver cells of patients with different types of mucopolysaccharidoses (Lapis, '79b; Phillips et al., '87). Characteristic storage material can also be demonstrated in alpha-1-antitrypsin deficiency (Callea et al., '84).

In Wilson's disease, a disorder of copper metabolism, excessive copper deposition can be recognized in the lysosomes as highly electron-dense deposits (Fig. 16A, B). X-ray microanalysis of liver tissue can help to prove the increased amount of copper in the liver biopsy (Fig. 16C). Another characteristic alteration in Wilson's disease is the great variety of mitochondrial shapes, forms, enlarged granules, and paracrystalline inclusions (Figs. 16D, 16E; Sternlieb, '80). Alterations in hepatic iron overload occur in hemosiderosis and hemochromatosis (Anderson and Rao, '86; Lapis, '79b; Phillips et al., '87; Searle et al., '87). Both ferritin and hemosiderin accumulate in cells as finely granular electron-dense material within membrane-bound siderosomes (Trump et al., '73; Fig. 17A) that derive from secondary lysosomes (Richter, '78). Disorders of pigment metabolism include the porphyrias. In addition to non-specific changes, such as fatty infiltrations, an increase in lipofuscin granules, focal necrosis, reactive hepatitis, hemosiderosis, mitochondrial alterations, and needle-shaped dense crystals arranged in a "starburst" pattern appear in erythropoietic porphyria (Lapis, '79a; Phillips et al., '87).

Unconjugated (Gilbert and Crigler-Najjar syndromes) and conjugated (Dubin-Johnson, Rotor syndromes, and Byler's disease) hyper-bilirubinemias are disorders of bilirubin metabolism. Different types of pigment granules accumulate in the liver in these disorders, especially lipofuscin granules in Gilbert's syndrome (Fig. 17C); highly electron-dense lysosomal granules in Dubin-Johnson syndrome (Fig. 17D); and "two-tone," fine granular pigments in Rotor syndrome (Fig. 17E; Barth et al., '71; Schaff et al., '69). Mitochondrial paracrystalline inclusions are common in hyperbilirubinemias (Schaff et al., '69), but they are non-specific and sensitive to proteolytic digestion (Schaff et al., '74a,b).

The liver can be involved in systemic amyloidosis (Phillips et al., '87). Fibers 7.5–10 nm in diameter appear in the Disse-space, causing atrophy of the hepatocytes (Fig. 17B). Fibrosis usually follows the deposition of amyloid (MacSween, '87).

CIRRHOSIS

Cirrhosis is a diffuse, progressive process in the liver with varying etiologies. It is characterized by fibrosis, distortion of architecture into abnormal nodules (Figs. 18A, 18C; Anthony et al., '77; Popper and Orr, '70), and by vascular abnormalities (Rappaport et al., '83). Electron microscopy has helped to discern more about the fibrogenesis process, which is one of the key problems

in the pathogenesis of cirrhotic liver (Lapis, '79c; Phillips et al., '87; Rojkind, '82). However, this method has not permitted the creation of a new or complete classification of this disease.

The "capillarization of the sinusoids" refers to the appearance of a basement-membrane-like material along the sinusoids accompanied by the deposition of collagen fibers and can be observed ultrastructurally (Fig. 18B; Bianchi et al., '84; Schaffner and Popper, '63). The widening of intercellular spaces between hepatocytes and the appearance of abnormal microvilli at the lateral surfaces are indices of disarranged trabecular architecture (Fig. 19A). The formation of bile canaliculi by more than two adjacent hepatocytes is a common feature of this condition (Fig. 19B). Degenerative and necrotic changes, as well as the deposition of bile and other pigments, can be readily observed (Fig. 19C). However, organelle ultrastructure is generally well preserved. In active cirrhosis the inflammatory cells are in especially close contact with the hepatocytic membrane (Fig. 19C).

LIVER TUMORS OF HEPATOCELLULAR ORIGIN

Electron microscopy permits the differentiation of primary and secondary liver tumors, since it distinguishes features indicative of the hepatic origin of the tumor, for example, bile canaliculi, bile pigment, sinusoid formation, and the like (Ghadially, '85; Tanikawa, '79). Benign liver tumors and tumor-like lesions include adenoma and focal nodular hyperplasia (Schaff et al., '86b). In both tumors the epithelial cells comprising the tumor mass closely resemble normal hepatocytes (Fig. 20A). However, giant mitochondria containing paracrystalline inclusions (Schaff et al., '86b), an excessive amount of glycogen, and damaged sinusoidal walls are common in adenomas (Figs. 20A, 20B). Several layers of basal membrane-like material can often be observed along the sinusoids (Fig. 20B). The portal areas and bile ducts are absent.

The cells comprising focal nodular hyperplasia appear normal by electron microscopy. However, as in adenoma, basal membrane formation along the sinusoids is common, and the blood vessels are surrounded by several layers of basal-membrane-like material (Fig. 20D). The proliferation of bile ducts is usually accompanied by inflammatory cells; the proliferating cells form abnormal bile ducts; and their cytoplasm is electron dense (Fig. 20C). Most investigators do not consider focal nodular hyperplasia as a true neoplasm but, rather, as a reaction of liver tissue to injury with prominent vascular changes (Christopherson et al., '77; Balazs, '76).

Hepatoblastomas have been divided into two types, epithelial and mixed epithelial-mesenchymal, and they have several characteristics indicative of hepatocellular origin (Gonzales-Crussi et al., '82; Ishak and Glunz, '67). These include round nuclei with finely dispersed chromatin (Fig. 21A), prominent rough endoplasmic reticulum (Figs. 21A–C), and numerous free ribosomes that form small groups. The mitochondria are typical of hepatocytes and may contain inclusions (Fig. 21A). Bile canaliculi with numerous (Fig. 21A) or

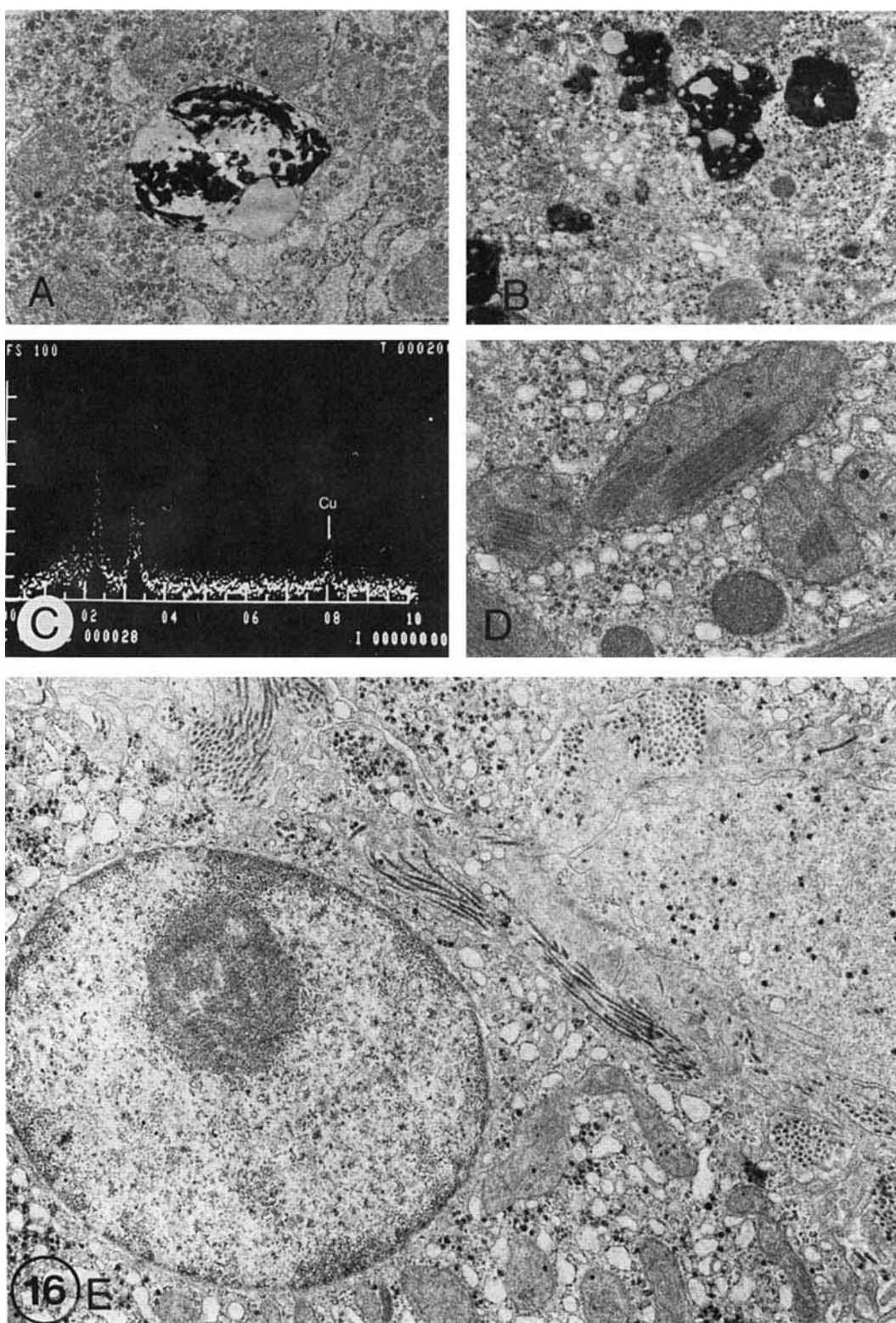


Fig. 16. Metabolic diseases: **A,B:** Wilson's disease; electron-dense deposits in the lysosomes. **C:** X-ray microanalysis shows copper deposit. **D:** Paracrystalline inclusions in mitochondria. **E:** Collagen fibers in the Disse space. **A:** $\times 16,000$; **B:** $\times 8,000$; **D:** $\times 16,500$; **E:** $\times 11,000$.

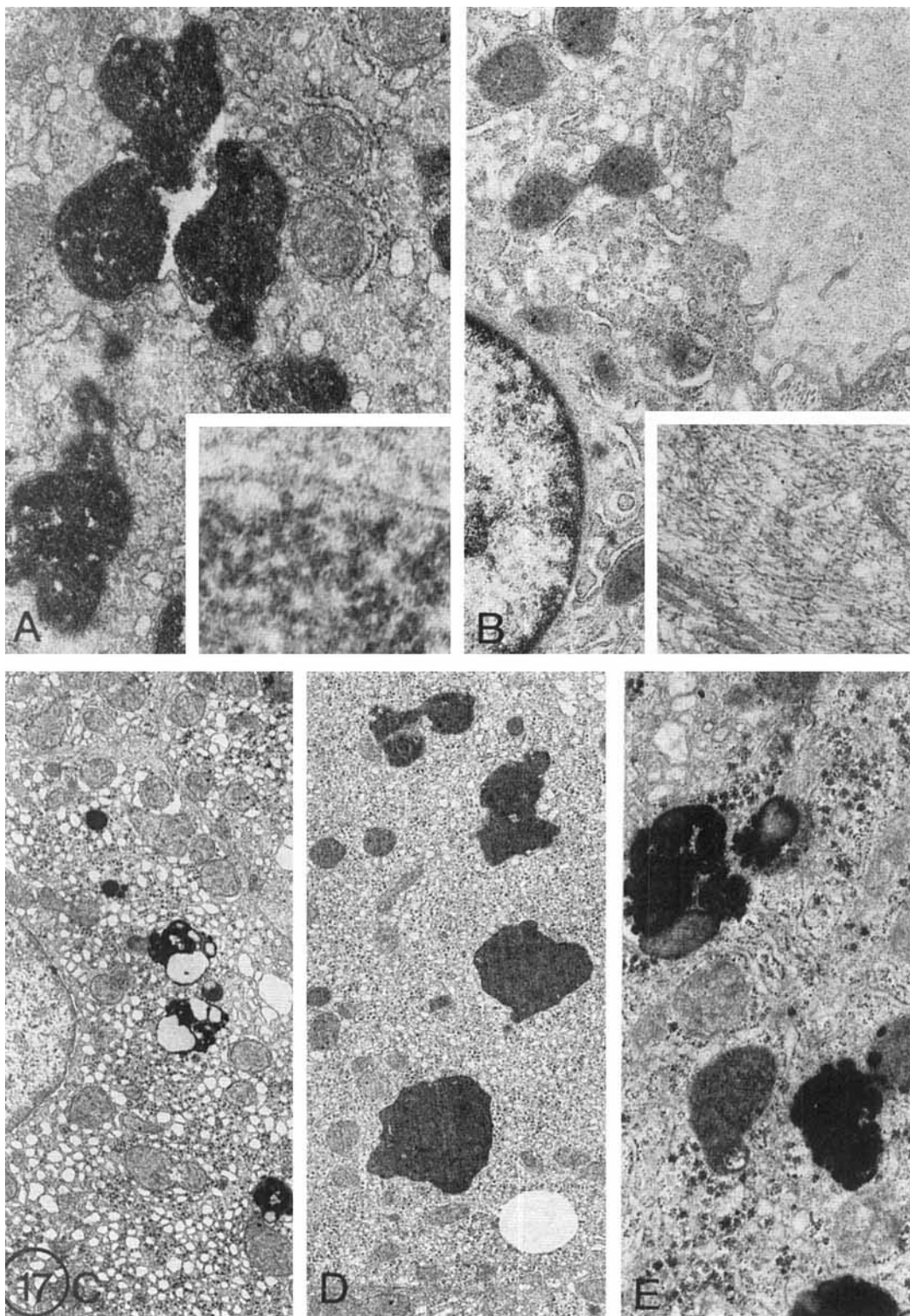


Fig. 17. Metabolic diseases. **A:** Hemosiderosis; hemosiderin granules with fine granular material. **Inset:** the granular material at higher magnification. **B:** A large amount of amyloid fibrils are deposited in the Disse space. **Inset:** the amyloid fibrils at higher

magnification. **C:** Pigment granules in Gilbert's disease; **D:** Dubin-Johnson syndrome; and **E:** Rotor syndrome. **A:** $\times 16,500$, **Inset:** $\times 40,000$; **B:** $\times 12,000$, **Inset:** $\times 33,000$; **C:** $\times 6,600$; **D:** $\times 6,600$; **E:** $\times 16,500$.

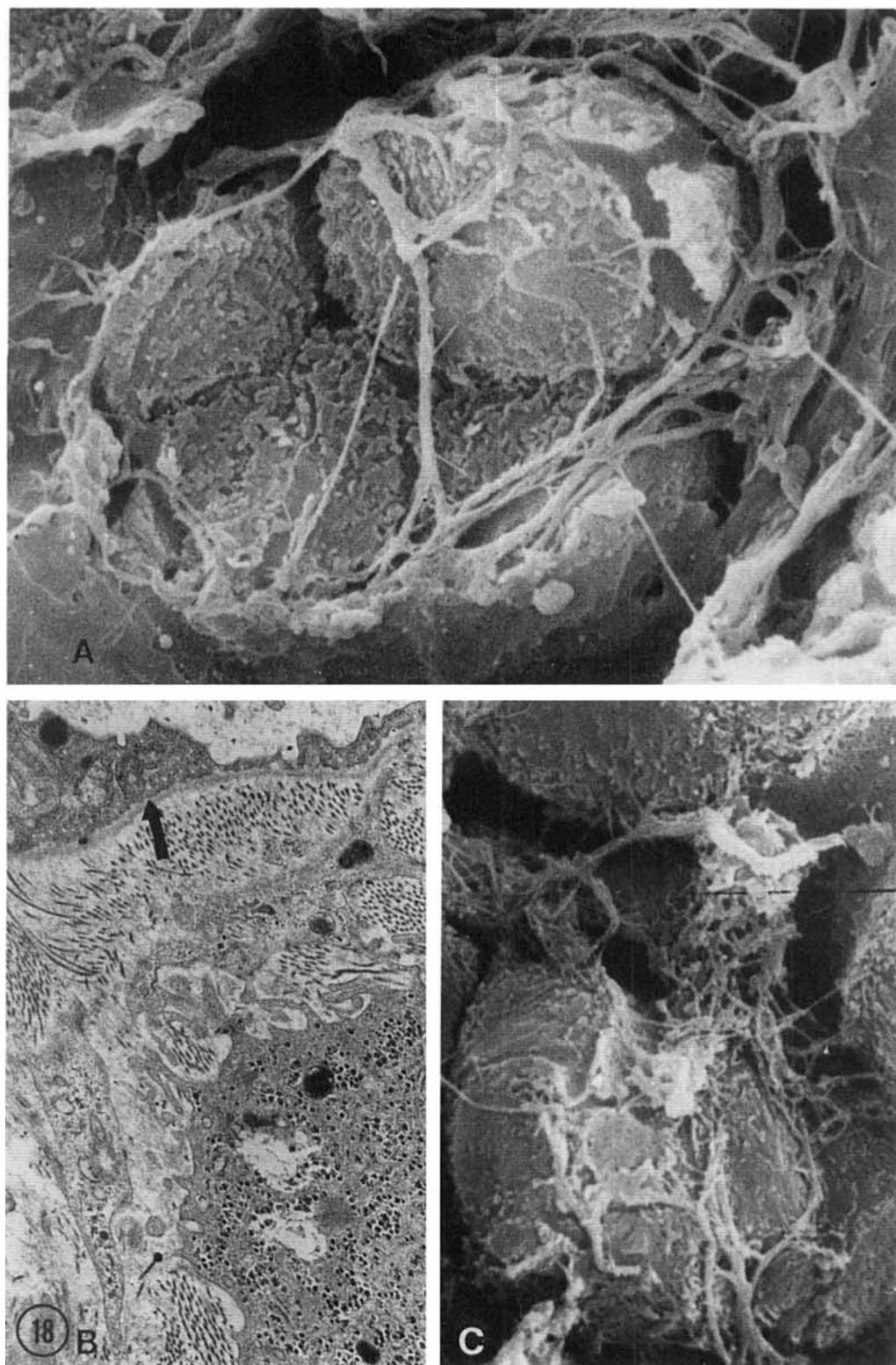


Fig. 18. Cirrhosis. **A,C:** Thick bundles of collagen fibers surround the abnormal lobules as seen by scanning electron microscopy. **B:** Collagen fibers, basal membrane-like material (arrow) along the sinusoids. **A:** $\times 8,000$; **B:** $\times 9,600$; **C:** $\times 8,000$.

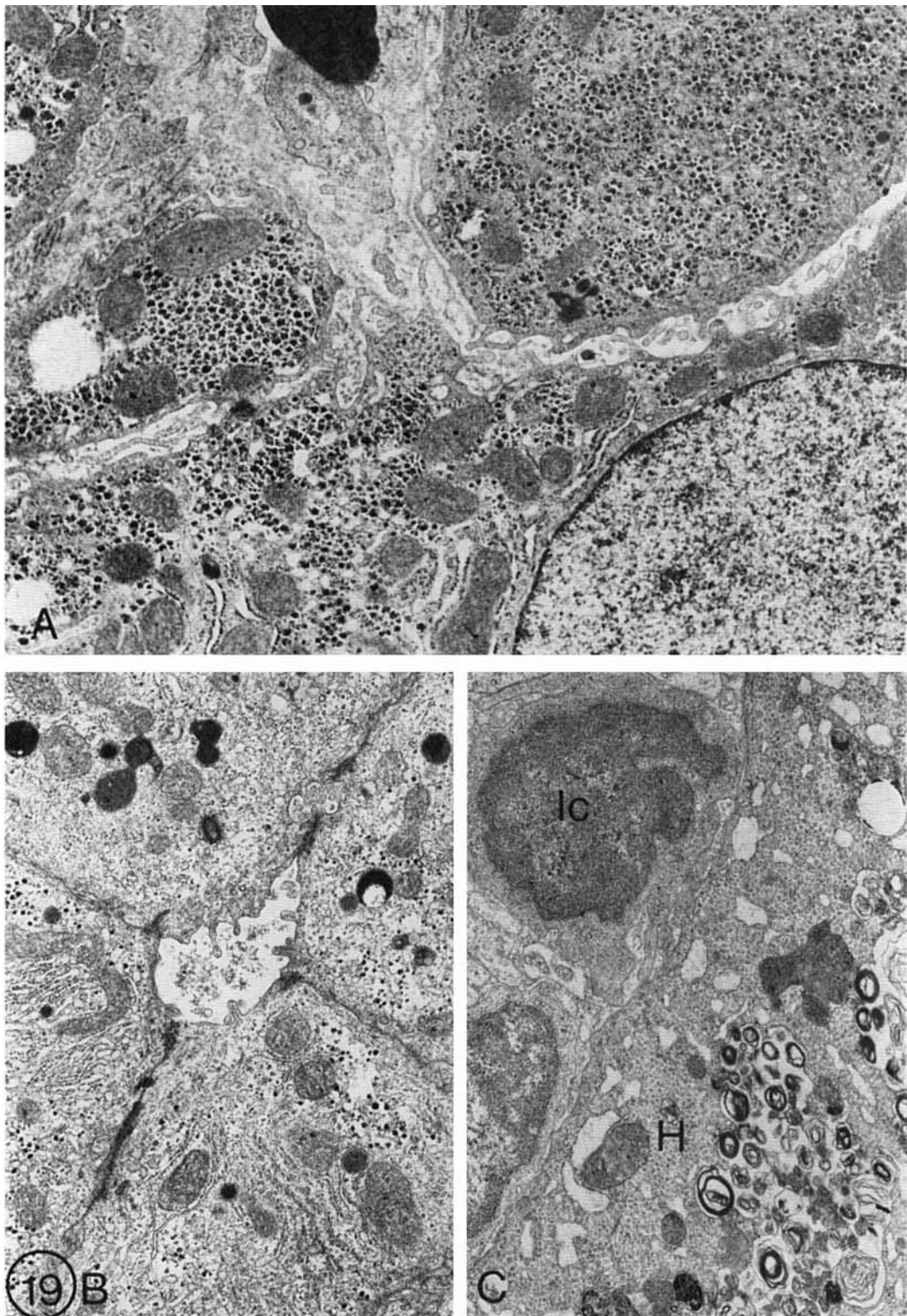


Fig. 19. Cirrhosis. **A:** Widening of intercellular space with microvilli. **B:** Bile canalculus formed by four hepatocytes. **C:** Lymphoid

cells (lc) in close contact with a hepatocyte (H). **A:** $\times 12,500$; **B:** $\times 8,000$; **C:** $\times 8,000$.

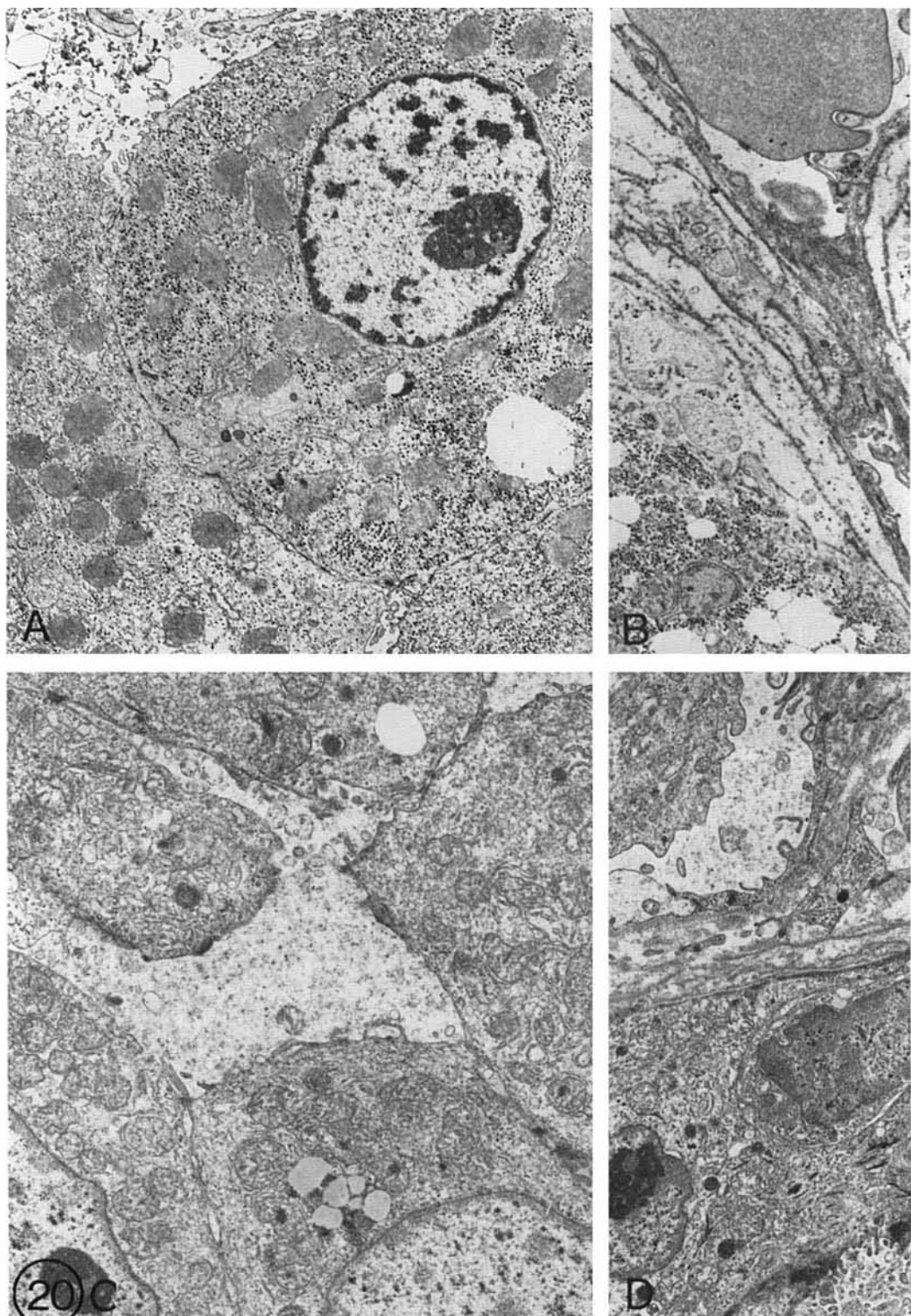


Fig. 20. Benign liver tumors. **A:** Adenoma; normal arrangement of organelles. **B:** Several layers of basal-membrane-like material around the blood vessels. **C:** Focal nodular hyperplasia; proliferating

bile ductular cells. **D:** Fragmented basal membrane around the blood vessels and ductular cells. **A:** $\times 6,600$; **B:** $\times 6,600$; **C:** $\times 6,600$; **D:** $\times 6,600$.

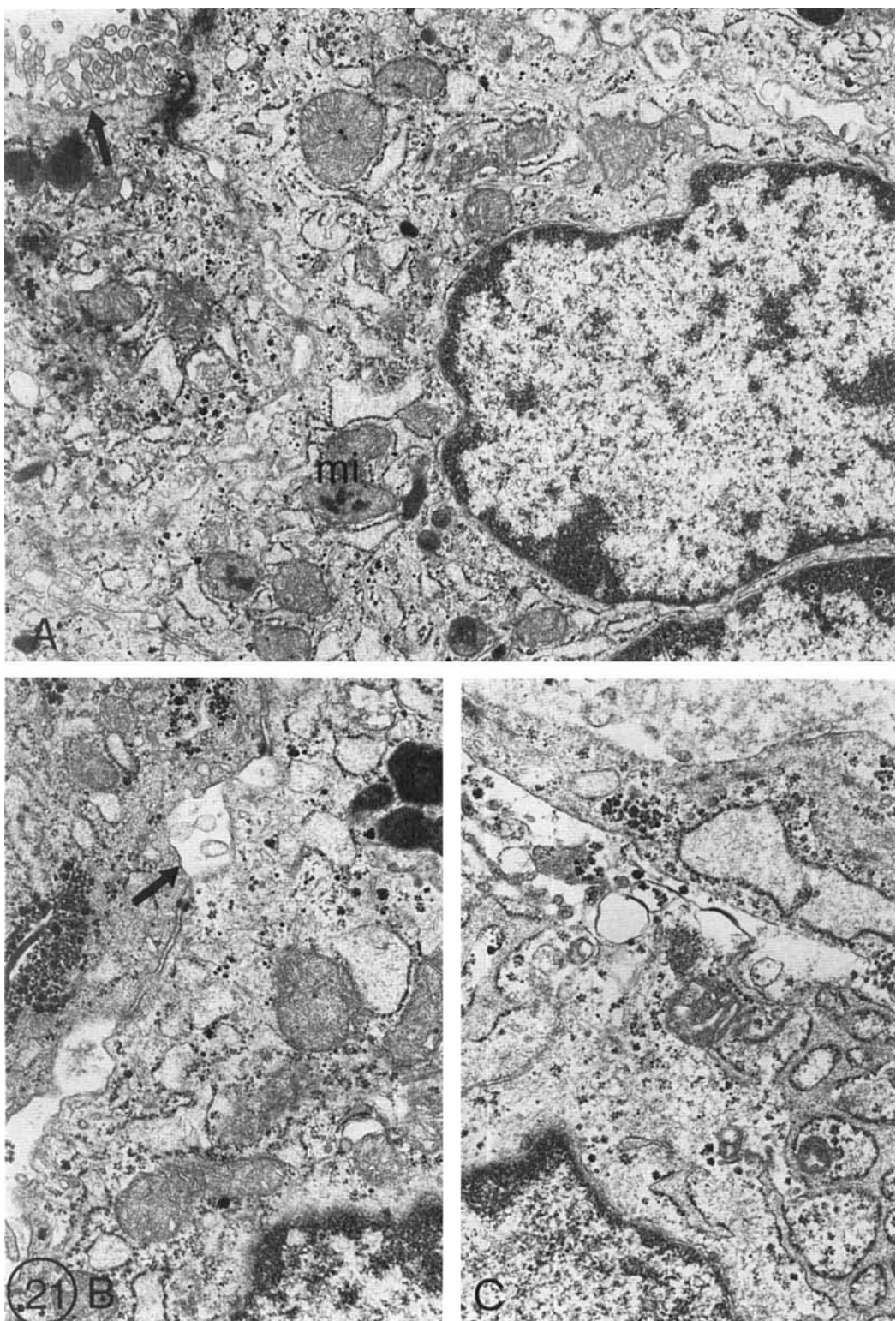


Fig. 21. Hepatoblastoma: epithelial type. **A,B:** Bile canaliculi (arrow), with prominent rough endoplasmic reticulum and numerous mitochondria (mi). **C:** Disse-space-like formation in the tumor. **A:** $\times 15,000$; **B:** $\times 20,000$; **C:** $\times 20,000$.

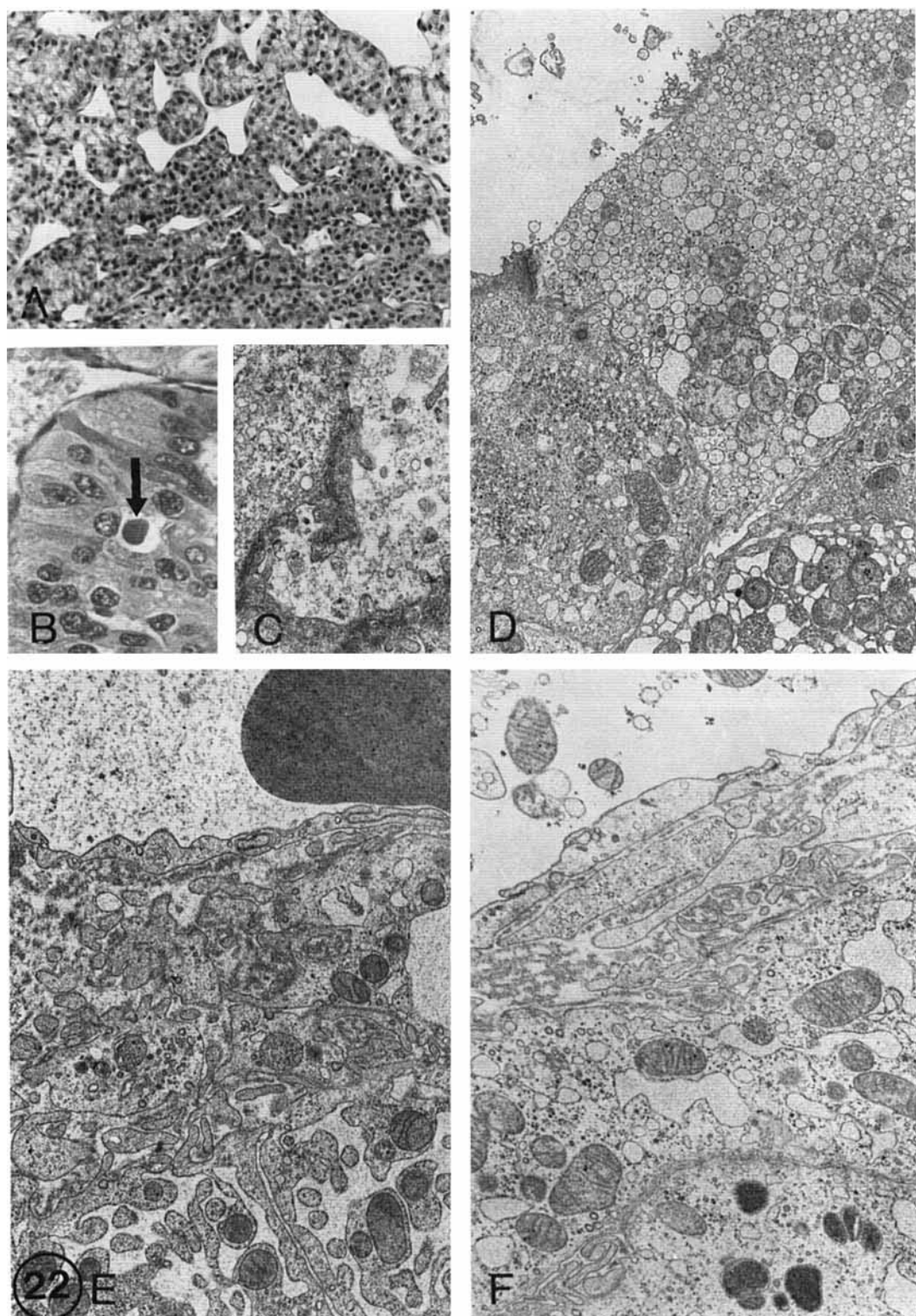


Fig. 22. Hepatocellular carcinoma. **A:** Well-differentiated tumor by light microscopy. **B:** Canalculus filled with bile plug (arrow). **C:** Bile canalculus surrounded by thickened ectoplasm and abnormal microvilli. **D:** Trabecular arrangement of tumor cells. **E,F:** Disse-

space-like formation filled with fragmented basal membrane-like material and cell processes. **A:** $\times 150$; **B:** $\times 350$; **C:** $\times 10,000$; **D:** $\times 6,000$; **E:** $\times 8,700$; **F:** $\times 9,900$.

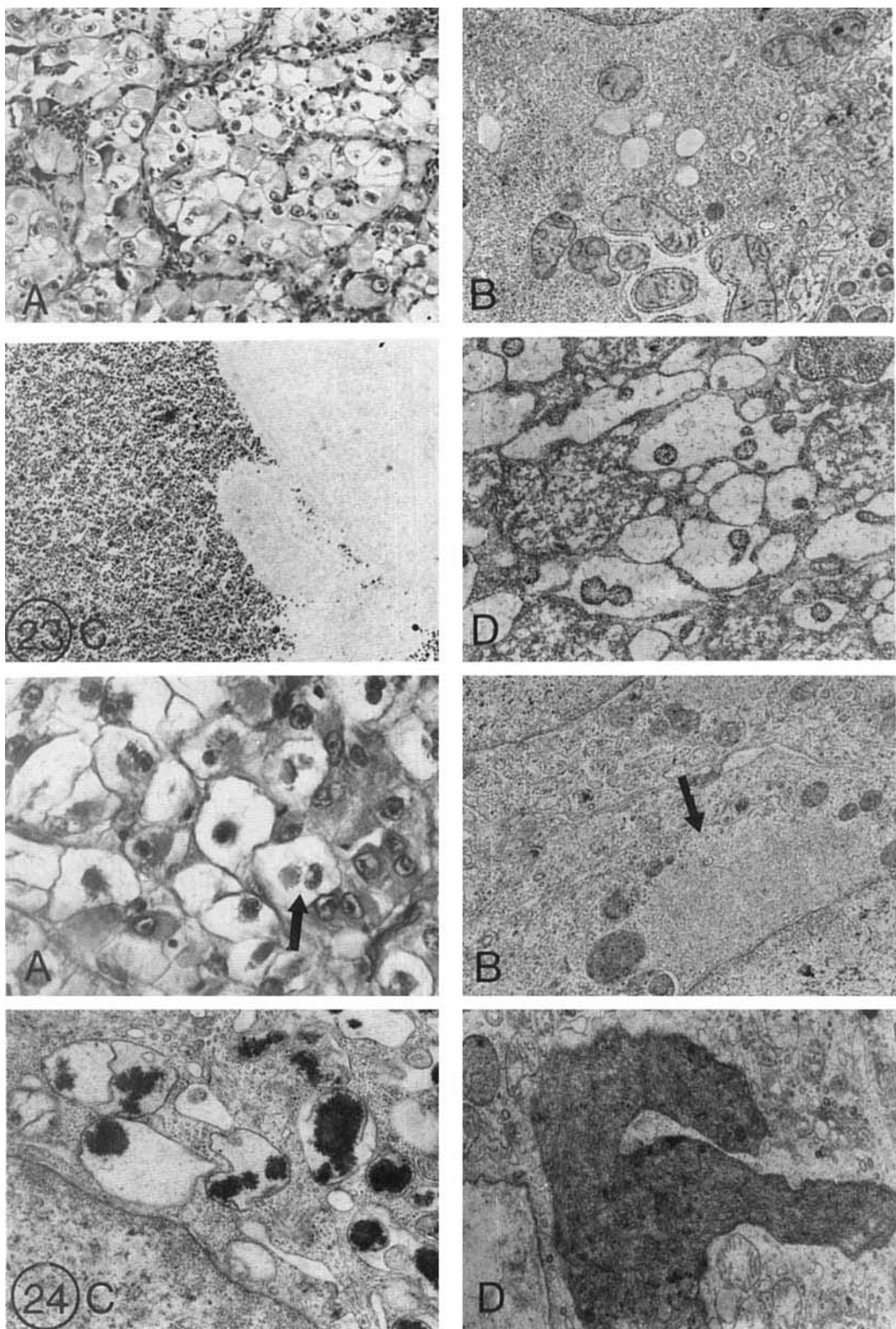


Fig. 23. Hepatocellular carcinoma: clear cell type. **A:** Clear cells by light microscopy; **B:** increased amount of glycogen; **C:** stained by silver proteinate; **D:** dilation of rough endoplasmic reticulum. **A:** $\times 200$; **B:** $\times 8,000$; **C:** $\times 8,000$; **D:** $\times 16,500$.

Fig. 24. Hepatocellular carcinoma: intracytoplasmic inclusions. **A:** Clear cells containing inclusions seen by light microscopy; **B:** fine granular inclusions (arrow); **C:** mitochondrial inclusions; **D:** abnormal giant mitochondrion. **A:** $\times 350$; **B:** $\times 8,900$; **C:** $\times 20,000$; **D:** $\times 12,000$.

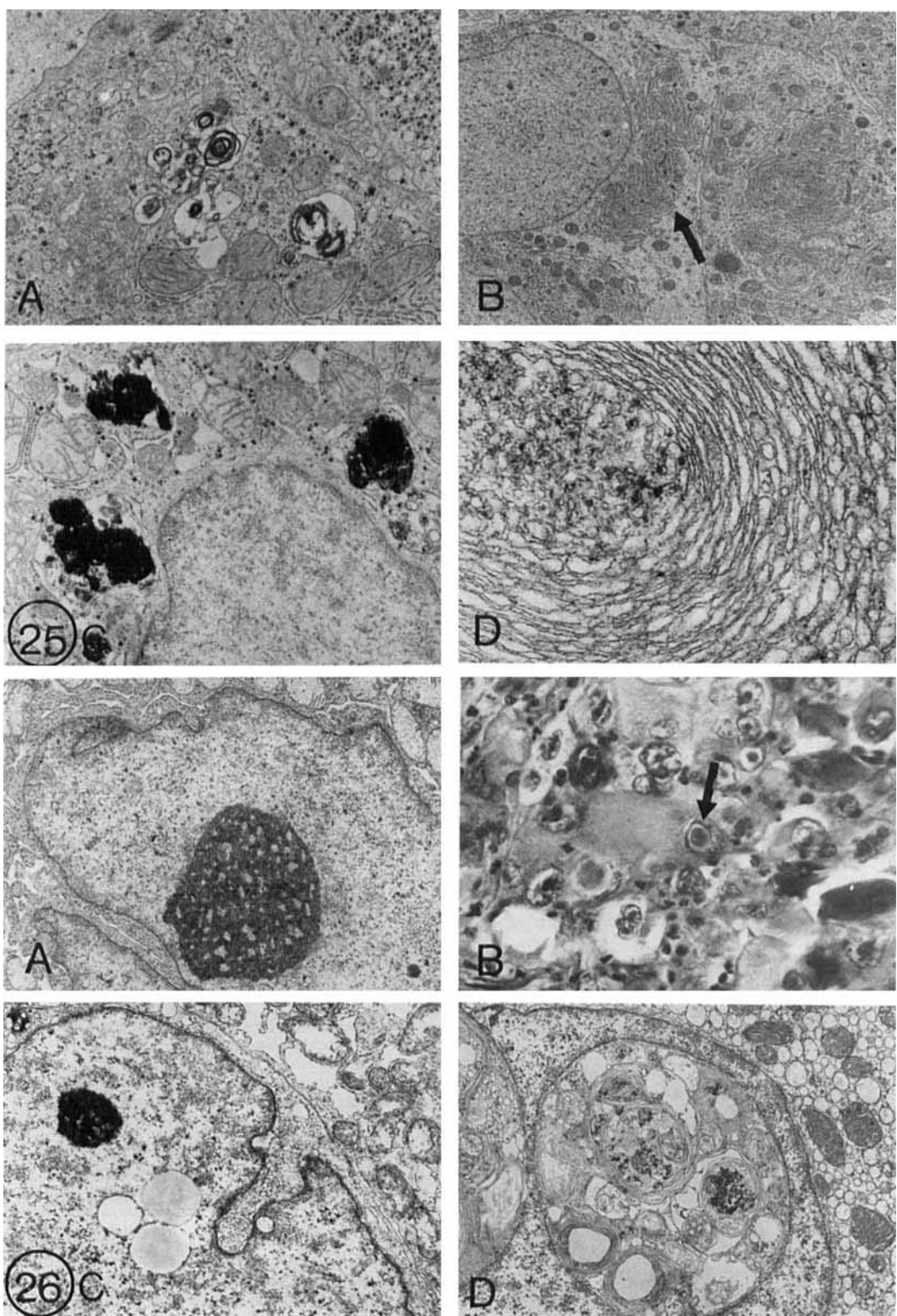


Fig. 25. Hepatocellular carcinoma: intracytoplasmic inclusions; **A**: Bile pigment; **B**: fingerprint-like arrangement (arrow) of rough and smooth endoplasmic reticulum membranes; **C**: Hemosiderin granules in tumor cells. **A**: $\times 8,900$; **B**: $\times 4,000$; **C**: $\times 10,000$; **D**: $\times 20,000$.

Fig. 26. Hepatocellular carcinoma. **A**: Large nucleolus; **B**: intranuclear inclusion by light microscopy (arrow); **C**: nuclear invagination and intranuclear lipid droplets; **D**: large intranuclear inclusion containing material of cytoplasmic origin. **A**: $\times 10,000$; **B**: $\times 350$; **C**: $\times 8,000$; **D**: $\times 10,000$.

few (Fig. 21B) microvilli are common. Although tumor cells may form Disse-space-like arrangements (Fig. 21C), other areas of the tumor are less well differentiated and consist of cells that do not resemble hepatocytes or fetal liver cells.

The histologic pattern of primary hepatocellular carcinoma may be well developed, moderately developed, or undeveloped (Anthony, '87; Lapis and Johannessen, '79; Peters, '76). The trabecular arrangement of hepatocytes may be well preserved (Figs. 22A, 22D). However, abnormally large bile canaliculi formed by several tumor cells is a common feature (Figs. 22B-D). Abnormal canalicular microvilli with dense pericanalicular ectoplasm can be seen (Fig. 22C). Bile pigment may accumulate in the dilated canaliculi (Figs. 22B, 22C) or in the cytoplasm of tumor cells (Fig. 25A). Furthermore, tumor cells and multilayered endothelial cells may form Disse-space-like channels (Fig. 22E,F). Clear cell carcinomas (Fig. 23A) contain large amounts of glycogen, often in monoparticulate form (Fig. 23C). Vesicularization (Fig. 23B) and "papillarization" of the endoplasmic reticulum (Fig. 23D) may contribute to the "clearness" of cytoplasm. Cytoplasmic inclusions detected by light microscopy (Fig. 24A) may represent fine, granular, proteinaceous material (Fig. 24B); enlarged, abnormal mitochondria (Figs. 24C, 24D); or fingerprint-like whorls of rough (Fig. 25B) or smooth (Fig. 25D) endoplasmic reticulum. Mitochondria may contain either granules or dense amorphous material (Fig. 24C; Schaff et al., '71). Different pigment granules such as bile pigment (Fig. 25A) or siderosomes (Fig. 25C) may appear also in the tumor cells.

Abnormalities of the nuclei and nucleoli may be very prominent (Schaff et al., '71). The nucleus may have an irregular profile (Fig. 26A) with cytoplasmic invaginations (Fig. 26C) and pseudoinclusions containing material of cytoplasmic origin (Fig. 26B, 26D). Fibrolamellar liver carcinoma has distinct light microscopic and ultrastructural features (Anthony, '87; Craig et al., '80). The enlarged tumor cells contain a large number of swollen, closely packed mitochondria, a feature that is also characteristic of oncocytes (Letkowitch et al., '80; Phillips et al., '87).

All of the alterations in hepatic ultrastructure described above may serve to establish the diagnosis, to reveal the etiologic agent(s) causing the liver disease, or to permit a better understanding of the pathogenesis of several common liver pathologies.

REFERENCES

- Anderson, W.R., and Rao, K.V. (1986) Hepatic iron overload in renal transplant recipients. *Ultrastruct. Pathol.*, 10:227-234.
- Anthony, P.P. (1987) Tumours and tumour-like lesions of the liver and biliary tract. In: *Pathology of the Liver*. R.N.M. MacSween, P.P. Anthony and P.J. Scheuer, eds. Churchill Livingstone, Edinburgh, pp. 574-645.
- Anthony, P.P., Ishak, K.G., Nayak, N.C., Poulsen, H.E., Scheuer, P.J., and Sabin, L.H. (1977) The morphology of cirrhosis: Definition, nomenclature and classification. *Bull. WHO*, 55:521-524.
- Arias, I.M., Popper, H., Schachter, D., and Shafritz, D.A. eds (1982) *The Liver: Biology and Pathobiology*. Raven Press, New York.
- Balázs, M. (1976) Electron microscopic study of benign hepatoma in a patient on oral contraceptives. *Beitr. Pathol.*, 159:299-306.
- Barth, R.F., Grimley, P.M., Berk, P.D., Bloomer, J.R., and Howe, R.B. (1971) Excess lipofuscin accumulation in constitutional hepatic dysfunction (Gilbert's syndrome). *Arch. Pathol.*, 91:41-47.
- Bianchi, L. (1970) Morphologic features in biopsy diagnosis of acute viral hepatitis. In: *Progress in Liver Diseases*. H. Popper and F. Schaffner, eds. Grune & Stratton, New York, Vol. III, pp. 236-251.
- Bianchi, F.B., Biagini, G., Ballardini, G., Genacchi, G., Faccani, A., Pisi, E., Laschi, R., Liotta, L., and Garbisa S. (1984) Basement membrane production by hepatocytes in chronic liver disease. *Hepatology*, 4:1167-1172.
- Callea, F., Fevery, J., and Desmet, V.J. (1984) Simultaneous alpha-1-antitrypsin accumulation in liver and pancreas. *Hum. Pathol.*, 15:293-295.
- Christopherson, W.M., Mays, E.T., and Barrows, G. (1977) A clinicopathologic study of steroid related liver tumors. *Am. J. Surg. Pathol.*, 1:31-41.
- Craig, J.R., Peters, R.L., Edmondson, H.A., and Omata, M. (1980) Fibrolamellar carcinoma of the liver: A tumor of adolescents and young adults with distinctive clinicopathologic features. *Cancer*, 46:373-379.
- Denk, H., and Franke, W.W. (1982) Cytoskeletal filaments. In: *The Liver: Pathology and Pathobiology*. I.M. Arias, H. Popper, D. Schachter, and D.A. Shafritz, eds. Raven Press, New York, pp. 55-71.
- Desmet, V.J. (1987) Cholestasis: Extrahepatic obstruction and secondary biliary cirrhosis. In: *Pathology of the Liver*. R.N.M. MacSween, P.P. Anthony, and P.J. Scheuer, eds. Churchill-Livingstone, Edinburgh, Ed. 2, pp. 364-423.
- Franke, W.W., Denk, H., Schmid, E., Osborne, M., and Weber, K. (1979) Ultrastructural, biochemical and immunologic characterization of Mallory bodies in livers of griseofulvin-treated mice. *Lab. Invest.*, 40:207-226.
- Galambos, J.T. (1985) Epidemiology of alcoholic liver disease in the United States of America. In: *Alcoholic Liver Disease*. P. Hall, ed. Edward Arnold, London, pp. 230-249.
- Ghadially, F.N. (1985) *Diagnostic Electron Microscopy of Tumors*. Butterworths, London.
- Gonzales-Crussi, F., Upton, M.P., and Maurer, H.S. (1982) Hepatoblastoma: Attempt at characterization of histologic subtypes. *Am. J. Surg. Pathol.*, 7:599-612.
- Hall, P. (1987) Alcoholic liver disease. In: *Pathology of the Liver*. R.N.M. MacSween, P.P. Anthony, and P.J. Scheuer, eds. Churchill Livingstone, Edinburgh, pp. 281-309.
- Ishak, K.G. (1973) Viral hepatitis: The morphologic spectrum. In: *The Liver*. E.A. Gall and F.K. Mostofi, eds. Williams & Wilkins, Baltimore, pp. 218-269.
- Ishak, K.G. (1982) The Liver. In: *Pathology of Drug-Induced and Toxic Diseases*. R.H. Riddel, ed. Churchill Livingstone, New York, pp. 457-513.
- Ishak, K.G., and Glunz, P.R. (1967) Hepatoblastoma and hepatocarcinoma in infancy and childhood. *Cancer*, 20:396-422.
- Ishak, K.G., and Sharp, H.L. (1987) Metabolic errors and liver disease. In: *Pathology of the Liver*. R.N.M. MacSween, P.P. Anthony, and P.J. Scheuer, eds. Churchill Livingstone, Edinburgh, London, pp. 99-180.
- Iwarson, S., Schaff, Z., Seto, B., Norkrans, G., and Gerety, R.J. (1985) Retrovirus-like particles in hepatocytes of patients with transfusion-acquired non-A, non-B hepatitis. *J. Med. Virol.*, 16:37-45.
- Jackson, D., Tabor, E., and Gerety, R.J. (1979) Acute non-A, non-B hepatitis: Specific ultrastructural alterations in endoplasmic reticulum of infected hepatocytes. *Lancet*, 1:1249-1250.
- Jezequel, A.M., and Orlandi, F. (1972) Fine morphology of the human liver as a tool in clinical pharmacology. In: *Liver and Drugs*. F. Orlandi and A.M. Jezequel, eds. Academic Press, London, pp. 145-192.
- Knight, J.A., and Wu, J.T. (1982) Screening profile for detection of inherited metabolic diseases. *Lab. Med.* 13:681-687.
- Kostianovsky, M., Orenstein, J.M., Schaff, Z., and Grimley, P.M. (1987) Cytomembranous inclusions observed in acquired immunodeficiency syndrome. *Arch. Pathol. Lab. Med.*, 111:218-223.
- Lapis, K. (1979a) Normal liver. In: *Electron Microscopy in Human Medicine*. Vol. 8. *The Liver*. J.V. Johannessen, ed. MacGraw-Hill, New York, pp. 3-19.
- Lapis, K. (1979b) Metabolic disorders. In: *Electron Microscopy in Human Medicine*. Vol. 8. *The Liver*. J.V. Johannessen, ed. McGraw-Hill, New York, pp. 20-79.
- Lapis, K. (1979c) Cirrhosis. In: *Electron Microscopy in Human Medicine*. Vol. 8. *The Liver*. J.V. Johannessen, ed. McGraw-Hill, New York, pp. 158-187.
- Lapis, K., and Johannessen, J.V. (1979) Pathology of primary liver

- cancer. In: *Liver Carcinogenesis*. K. Lapis and J.V. Johannessen, eds. Hemisphere, Washington, DC, pp. 145–185.
- Lapis, K., and Schaff, Z. (1979) Acute viral hepatitis. In: *Electron Microscopy in Human Medicine*, Vol. 8. The Liver. J.V. Johannessen, ed. McGraw-Hill, New York, pp. 124–136.
- Letkowitch, J.H., Arborgh, B.A.M., and Scheuer, P.J. (1980) Oxyphilic granular hepatocytes: Mitochondrial-rich liver cells in hepatic disease. *Am. J. Clin. Pathol.*, 74:432–441.
- MacSween, R.N.M. (1987) Liver pathology associated with diseases of other organs. In: *Pathology of the Liver*. R.N.M. MacSween, P.P. Anthony, and P.J. Scheuer, eds. Churchill Livingstone, Edinburgh, pp. 646–688.
- MacSween, R.N.M., and Burt, A.D. (1986) Histologic spectrum of alcoholic liver disease. *Semin. Liver Dis.*, 6:221–232.
- MacSween, R.N.M., and Scuthorne, R.J. (1987) Developmental anatomy and normal structure. In: *Pathology of the Liver*. R.N.M. MacSween, P.P. Anthony, and P.J. Scheuer, eds. Churchill Livingstone, Edinburgh, pp. 1–46.
- Motta, P.M., and Fujita, T. (1978) *The Liver: An Atlas of Scanning Electron Microscopy*. Igaku-Shoin, Tokyo.
- Peters, R.L. (1976) Pathology of hepatocellular carcinoma. In: *Hepatocellular Carcinoma*. K. Okuda and R.L. Peters, eds. Wiley, New York, pp. 107–168.
- Peters, S.P., Lee, R.E., and Glew, R.H. (1977) Gaucher's disease: A review. *Medicine*, 56:425–442.
- Phillips, M.J., Poucels, S., Patterson, J., and Valencia, P. (1987) *The Liver: An atlas and Text of Ultrastructural Pathology*. Raven Press, New York.
- Popper, H. (1975) Clinical pathologic correlation in viral hepatitis. *Am. J. Pathol.*, 81:609.
- Popper, H. (1986) General pathology of the liver: Light microscopic aspects serving diagnosis and interpretation. *Semin. Liver Dis.*, 6:175–184.
- Popper, H., and Orr, W. (1970) Current concepts in cirrhosis. *Scand. J. Gastroenterol.*, 5(suppl. 6):203–222.
- Popper, H., and Schaffner, F. (1963) Fine structural changes of the liver. *Ann. Intern. Med.*, 59:674–691.
- Popper, H., Thung, S.N., and Gerber, M.A. (1981) Pathology of alcoholic liver diseases. *Semin. Liver Dis.*, 1:203–216.
- Rappaport, A.M., Borowy, Z.J., Lougheed, W.M., and Lotto, W.N. (1954) Subdivision of hexagonal liver lobules into a structural and functional unit: Role in hepatic physiology and pathology. *Anat. Rec.*, 119:11–34.
- Rappaport, A.M., MacPhee, P.J., Fischer, M.M., and Phillips, M.J. (1983) The scarring of the liver acini (cirrhosis). *Virchows Arch. [A]*, 402:107–137.
- Richter, G.W. (1978) The iron-loaded cell—the cytopathology of iron storage. *Am. J. Pathol.*, 91:362–404.
- Rojkind, M. (1982) Fibrogenesis: Biology and pathobiology. In: *The Liver: Biology and Pathobiology*. I.M. Arias, H. Popper, D. Schachter, and D.A. Shafritz, eds. Raven Press, New York, pp. 801–809.
- Rouiller, C. (1957) Contribution de la microscopie électronique à l'étude du foie normal et pathologique. *Ann. Anat. Pathol.*, 2:548–561.
- Schaff, Z., Gerety, R.J., Grimley, P.M., Iwarson, S.A., Jackson, D.R., and Tabor, E. (1985) Ultrastructural and cytochemical study of hepatocytes and lymphocytes during experimental non-A, non-B hepatitis in chimpanzees. *J. Exp. Pathol.*, 2:25–36.
- Schaff, Z., Hoofnagle, J.H., and Grimley, P.M. (1986a) Hepatic inclusions during interferon therapy in chronic viral hepatitis. *Hepatology*, 6:966–970.
- Schaff, Z., and Lapis, K. (1979a) Cholestasis. In: *Electron Microscopy in Human Medicine*. Vol. 8. The Liver. J.V. Johannessen, ed. McGraw-Hill, New York, pp. 80–88.
- Schaff, Z., and Lapis, K. (1979b) Injury by drugs and toxins. In: *Electron Microscopy in Human Medicine*. Vol. 8. The Liver. J.V. Johannessen, ed. McGraw-Hill, New York, pp. 89–115.
- Schaff, Z., Lapis, K., and André, J. (1974a) Study of the tridimensional structure of intramitochondrial crystalline inclusions. *J. Microsc.*, 20:259–264.
- Schaff, Z., Lapis, K., and André, J. (1974b) Effect of proteolytic digestion on mitochondrial crystalline inclusions in Gilbert's syndrome. *J. Microsc.*, 20:265–270.
- Schaff, Z., Lapis, K., and Henson, D.E. (1986b) Liver. In: *The Pathology of Incipient Neoplasia*. D.E. Henson and J. Albores-Saavedra, eds. W.B. Saunders, Philadelphia, pp. 167–202.
- Schaff, Z., Lapis, K., Kereszty, S., Kolláth, Z., Hollós, I. (1982) Occurrence of tubuloreticular inclusions in acute viral hepatitis. *Ultrastruct. Pathol.*, 3:169–173.
- Schaff, Z., Lapis, K., and Sáfrány, L. (1969) Feinstrukturelle Veränderungen der Leber bei der Gilbert-Krankheit. *Beitr. Pathol. Anat.*, 140:54–70.
- Schaff, Z., Lapis, K., and Sáfrány, L. (1971) The ultrastructure of primary hepatocellular cancer in man. *Virchows Arch. [A]*, 352:340–358.
- Schaff, Z., Seto, B., Coleman, W.G., Jr., and Lapis, K. (1986c) Morphology and immunohistochemistry of experimental and human non-A, non-B hepatitis. *Tokai J. Exp. Clin. Med.*, 11:(Suppl) 11–120.
- Schaff, Z., Tabor, E., Jackson, D.R., and Gerety, R.J. (1984) Ultrastructural alterations in serial liver biopsy specimens from chimpanzees experimentally infected with a human non-A, non-B hepatitis agent. *Virchows Arch. Cell Pathol.*, 45:301–312.
- Schaffner, F., and Popper, H. (1963) Capillarization of hepatic sinusoids in man. *Gastroenterology*, 44:239–242.
- Scheuer, P.J. (1987) Viral hepatitis. In: *Pathology of the Liver*. R.N.M. MacSween and P.J. Scheuer, eds. Churchill Livingstone, Edinburgh, pp. 202–224.
- Searle, J., Kerr, J.F.R., Halliday, J.W., and Powell, L.W. (1987) Iron storage disease. In: *Pathology of the Liver*. R.N.M. MacSween, P.P. Anthony, and P.J. Scheuer, eds. Churchill Livingstone, Edinburgh, pp. 181–201.
- Shimizu, Y.K., Feinstone, S.M., and Purcell, R.H. (1979) Non-A, non-B hepatitis: Ultrastructural evidence for two agents in experimentally infected chimpanzees. *Science*, 205:197–200.
- Simson, I.W., and Gear, J.H.S. (1987) Other viral and infectious diseases. In: *Pathology of the Liver*. R.N.M. MacSween, P.P. Anthony, and P.J. Scheuer, eds. Churchill Livingstone, Edinburgh, pp. 224–265.
- Sternlieb, I. (1980) Copper and the liver. *Gastroenterology*, 78:1615–28.
- Tanikawa, K. (1979) *Ultrastructural Aspects of the Liver and Its Disorders*. Igaku-Shoin, Tokyo.
- Trump, B.F., Kim, K.M., and Iseri, O.A. (1976) Cellular pathophysiology of hepatitis. *Am. J. Clin. Pathol. (suppl)* 65:828–835.
- Trump, B.F., Valigorsky, J.M., Arstila, A.U., Mergner, W.J., and Kinney, T.D. (1973) The relationships of intracellular pathways of iron metabolism to cellular iron overload and iron storage diseases. *Am. J. Pathol.*, 72:295–336.
- Wilson, J.H.P. (1986) Drug metabolism and the liver. In: *The Liver Annual*, Vol. 5. I.M. Arias, M. Frenkel, and J.H.P. Wilson, eds. Elsevier, Amsterdam, pp. 503–520.
- Zimmerman, H.J., and Ishak, K.G. (1987) Hepatic injury due to drugs and toxins. In: *Pathology of the Liver*. R.N.M. MacSween, P.P. Anthony, and P.J. Scheuer, eds. Churchill Livingstone, Edinburgh, pp. 503–573.
- Zuckerman, A.J. (1984) Viral hepatitis. In: *The Liver Annual*, Vol. 4. I.M. Arias, M. Frenkel, and J.H.P. Wilson, eds. Elsevier, Amsterdam, pp. 187–208.